Exploring stable carbon isotope analysis of fatty acids by GC-C-IRMS for local paleoenvironment reconstructions

Jose Agustin Cordero, Ramiro Javier March

Exploring stable carbon isotope analysis of fatty acids by GC-C-IRMS for local paleoenvironment reconstructions

José Agustín Cordero[1] & Ramiro J. March[2]

Abstract

The aim of this paper is to explore the feasibility of using $\delta^{13}C$ values of the fatty acid methyl esters (FAMEs) of $C_{16:0}$ and $C_{18:0,}$ extracted from archaeological bones of *Lama guanicoe* (guanaco), as a proxy data in paleoenvironmental reconstruction. Our aim is to determine the significance of these biomarkers for understanding the paleoenvironmental changes. We also investigate the relation between the fatty acids $\delta^{13}C$ values of bones and the archaeological cave sediments, which can have a natural and/or an anthropic origin. Using this approach, we cross-compare the $\delta^{13}C$ values of bones -which are then used as proxy data- with their corresponding archaeological soils to analyse their evolution and possible relations. The bones values are compared with different types of available palaeoenviromental data (like rodents distributions from Traful I and, Moreno Lake and Cordón Serrucho Norte pollen columns) to build up a regional paleoclimatic sequence. Finally, we propose three phytogeographical environment reconstructions (early, middle and late Holocene) for the study area.

Keywords: Patagonia, Holocene, Paleoenvironment, Molecular proxies, Compound specific $\delta^{13}C$, Gas chromatography combustion isotope ratio mass spectrometry (GC-C-IRMS), *Lama guanicoe*, soils.

[1] Centro de Investigaciones en Antropología Filosófica y Cultural (CIAFIC-CONICET), agustincordero74@gmail.com
[2] UMR6566 Centre de Recherche en Archéologie, Archéosciences et Histoire, Université de Rennes 1 - CNRS, Ramiro.March@univ-rennes1.fr

1. Introduction

The use of biomarkers as molecular proxies is a relatively recent application in paleoclimatology (Eglinton and Eglinton, 2008). The $\delta^{13}C$ values obtained from long-chain *n*-alkanes in leaf wax and saturated fatty acids in marine sediments have served firstly as a proxy indicating the type of vegetation and landscape, as well as climate evolution (Duan, et al., 1997, Rommerskirchen, et al., 2003, Rommerskirchen, et al., 2006, Zhang, et al., 2006). The same approach was developed also for lake sediments (Ficken, et al., 1998, Huang, et al., 2006, Huang, et al., 1999, Jacob, et al., 2004, Jacob, et al., 2007), and was recently applied to the study of continental basins (Zech, et al., 2009).

In archaeology, this technique has been applied to identify the origin of lipids in different archaeological contexts, mostly concerning ceramics, but has also been used for stones and soils related to cooking activities (Evershed, 2008, Evershed, et al., 2002, March, 1999, March and Lucquin, 2006, March, et al., 2012, Outram, et al., 2009, Spangenberg, et al., 2006), as well as in rock art paint residues (Boschin, et al., 2011, Boschín, et al., 2002, Maier, et al., 2007). Moreover, the $\delta^{13}C$ signatures of individual fatty acids ($C_{16:0} - C_{18:0}$) have been utilized for the study of trophic markers (Ruess and Chamberlain, 2010) and biotic interactions in complex ecosystems (Evans, et al., 2003). Finally, bulk analysis of $\delta^{13}C$ on tooth enamel has been used to address the seasonal variability of movement patterns and grazing behaviour in bison populations of the Great Plains (Widga, et al., 2010) as well as, for the management strategies of domestic stock (Balasse, et al., 2002, Balasse, et al., 2001, Balasse, et al., 2003, Makarewicz and Tuross, 2006, Tornero and Sana, 2011). These authors show that $\delta^{13}C$ values indicate C_3/C_4 diet, while $^{87}Sr/^{86}Sr$ ratios reflect seasonal movement.

Our aim is to explore the relation between the fatty acid composition of guanaco bones and the lipids of the cave's sediments, which may have a natural and/or an anthropic origin. We attempt to determine the significance and the confidences of these biomarkers in order to understand the paleoenvironmental changes. Using this approach, we cross-compare $\delta^{13}C$ values of individual fatty acid methyl esters (FAMEs) of chain-length $C_{16:0}$ and $C_{18:0}$ extracted from guanaco bones with the corresponding archaeological cave layers from Traful I (40° 43' S, 71°07' W) and Epullán Grande (43°23'S, 70°11' W). We compare our results with different kinds of available paleoenvironmental data (rodent's distributions and pollen columns) to propose a regional paleoclimatic sequence and a phytogeographical reconstruction of the landscapes near the Traful I and Epullán Grande caves. The ultimate goal is to establish an environmental framework that allows us to put into perspective the subsistence practices of the hunters-gatherers inhabiting the cave during the Holocene.

2. Study area description

The Traful I and Epullán Grande caves

Traful I cave is located on the eastern edge of the sub-Andean district of Patagonia (León, et al., 1998, see Figure 1), at the base of Cerro de las Chivas (Figure 2a) in the Nahuel Huapi National Park, about 760 m above sea level (Crivelli Montero, et al., 1993). The radiocarbon dates reported in Figure 2b[3] were calibrated with Calib Rev 6.0.1 (Reimer, et al., 2009). The Traful I cave represents **a unique locality** (Figure 1)

[3]Recently, new radiocarbon dates were obtained from jaw bones of *Ctenomys* sp. Chan, Y.L., Hadly, E.A., 2011. Genetics variation over 10 000 years in *Ctenomys*: comparative phylochronology provides a temporal perspective on rarity, envoromental change and demography, Molecular Ecology 20, 4592-4605, Chan, Y.L., Lacey, E.A., Pearson, O.P., Hadly, E.A., 2005. Ancient DNA reveals Holocene loss of genetic diversity in a South American rodent, Biology letters 1, 423-426.. However, it is difficult to use these dates for our purposes here. Layer 14 from ibid. should be assigned to layer 21 because the stratigraphy was defined by Crivelli Montero, E.A., Curzio, D., Silveira, M.J., 1993. La estratigrafía de la Cueva Traful I (provincia del Neuquén), Præhistoria 1, 9-160., and the authors based their work on a previous study, where the nomenclature of the layer was not revised.

containing valuable paleoenvironmental information and located in the limit of two different ecological zones, with a radiocarbon-dated sequence covering the past 10,000 years (Figure 2c). The initial occupations, which are dated at between 9,430 yr BP ± 230 (CA-2676) and 9,285 ± 105 yr BP (GX-1711G-AMS), can be regarded as short term. These occupations left some bones and lithic assemblages including a small core and several flakes, a few of which are retouched. Although component I (Unidad Traful), dated at between 7,855 ± 70 yr BP (LJ-5133) and 7,308 ± 285 yr BP (LP-8113), shows the same characteristics, the lithic assemblage also contains triangular projectile points, scrapers and some retouched tools. Component II A (Confluencia) represents the first major occupation of the site, dated at between 6,030 ± 115 yr BP (I-11304) and 6,240 ± 60 yr BP (LJ-5132). This occupation layer includes mostly basalt projectile points that are not pedunculated, some flakes and cores and a predominance of used flakes. These occupations are covered by layer 6 and layer 5 (tephra), both of which are sterile. Component IIB, dated between 2,720 ± 40 yr BP (LJ-5131) and 2,230 ± 40 yr BP (LJ-5131), reflects more limited and sporadic occupations, with stone tools showing some differences with the previous layer, but which nevertheless share their general features. We can observe here the appearance of leaves and forms with larger bases. Although the final occupations of hunters-gatherers, belonging to the most recent "ceramic-independent period" are of limited importance, they include evidence for the use of pedunculated projectile points (Crivelli Montero, et al., 1993). Even if the sequence at Traful I cave is extremely rich, the first occupations yield only a few bone fragments which are assigned to Artiodactyla (Cordero, 2011a). Therefore, we decided to include in this study a bone from the Epullán Grande cave (LL onwards), situated at a distance of about 86 km, which yields a similar age to the Traful occupations (Figure 1).

The LL stratum #07 is first choose to enlarge our time span. Stratum #07 covers most of the bedrock and includes: a hearth (#32) overlying the bedrock, which is dated at 9,970 ± 100 yr BP (LP-213) (Crivelli Montero, et al., 1996).

Recent studies of the faunal remains from the entire sequence of Traful I (Cordero, 2011a, Cordero, 2011b) and the firsts occupation of LL (Cordero, 2009) show that, at the beginning of the Holocene, two different economic strategies co-existed in north-western Patagonia. The first practised by guanaco hunters living on the steppe and using projectile points, extending as far as the ecotonal forest-steppe area, where a second group is found showing a simpler technology, using local lithic raw materials and exploiting mainly medium-sized and small game (hog-nosed skunks, two types of armadillos, two fox species, and lesser rhea), and scarcely any guanaco. Guanaco exploitation was widespread in the middle Holocene, both in the forest-steppe ecotone and on the steppe, but was always supplemented by small-sized fauna, vegetables, molluscs and fish. During the last 2,000 years, the diversity of exploited species has significantly increased (Cordero, 2012).

The present-day landscape of north-western Patagonia

The climate in Patagonia is governed by three important factors: the geography, the high and low pressure systems and the ocean currents. The Andean chains determine the rainfall on the east side of the continent. The moisture carried by the westerlies is precipitated as rain on the western slope of the Andean crest, making the air warmer and drier as it descends towards the steppe (Paruelo, et al., 2007, Paruelo, et al., 1998). In this way, central Patagonia receives less than 200 mm of precipitation per year. The track and intensity of cyclonic storms associated with the austral Westerlies is controlled by the strength and latitude of the subtropical anticyclone in the southeast

Pacific and the circum-Antarctic low-pressure belt (Aceituno, 1988, Aceituno, 1989). The interannual rainfall variability at 41°S is strongly related to the ENSO (El Niño Southern Oscillation) (Lamy, et al., 2001). Consequently, vegetation types follow the same west-east gradient of rainfall (León, et al., 1998). Hence, the north Patagonia landscape shows a phytogeographical transition from forests in the west, passing through grassy steppe to grassy shrub-steppe, and finally, the shrub-steppe and Monte district in the east (Figure 3a, modified after Pardiñas and Teta (In press)). Grasses and shrubs are the main components of the extensive plains and steppes of Patagonia.

The formation of the Andes Chain during the Miocene created the conditions for the drying wind and desertification. Because of this, the grasslands and steppes are heterogeneous, both physiognomically and floristically. The vegetation types reflect the limits imposed by the climate, topography and soil characteristics of each region (Paruelo, et al., 2007). Therefore, rangelands with shrubs make up communities that cover 60% or more of the territory of Patagonia, falling to 10% or less in drier areas. Originally, grasslands dominated the environment (Aguilar and Sala, 1998), but the proportion of grass is now tending to change in favour of shrub due to heavy grazing of domestic animals, with shrubland beginning to form part of the landscape since the early twentieth century (Bertiller and Bisigato, 1998).

The isotopic carbon cycle

The differential intake of plants with C_3 and C_4 photosynthetic pathways results in different carbon isotopic signatures (Pate 1994). Variations in the proportion of C_3/C_4 grasses are related to the increase in atmospheric CO_2 linked to climate change. This distribution of plant types not only impacts the primary productivity, but also the distribution, evolution and migration of vertebrates and invertebrates (Ehleringer, et al.,

1997). Studies of fossil herbivore teeth from the early and middle Miocene show that their diet was exclusively based on C_3 plants. But there was a change in the photosynthetic systems of terrestrial ecosystems during the late Miocene, leading to the establishment of the distribution patterns of C_3 and C_4 grasses as seen at present. The recent evolution of this distribution is reflected by a latitudinal gradient that first developed in the equatorial regions and then shifted to higher latitudes (MacFadden, et al., 1999, MacFadden, et al., 1996).

Currently, this distribution is not only latitudinal but also varies with elevation (Pate 1994). C_4 plants dominate the lower-lying zones, but decrease in abundance with increasing elevation. In the zone between 2000 and 2500 m, C_3 grasses are dominant (Cabido, et al., 1997, Cavagnaro, 1988). The overlap area where both types of species coexist in the same proportion occurs at different elevations (1500 m average) in other regions. Cabido et al. (1997) and Cavagnaro (1988) found that temperature is the most suitable variable for predicting this distribution. However, in contrast to Cavagnaro (1988), Cabido et al. (1997) suggest that precipitation also has a good correlation with C_3/C_4 plant distribution. This phenomenon can also be found in other desert areas worldwide, for example in Australia (Hattersley 1983) and Mongolia (Pyankov, et al., 2000). Experimental work has shown that increased summer rainfall produces a relative increase in C_4 plants because of their extensive and shallow root systems, which take more advantage of small rainfall events, thus improving the uptake of moisture (Skinner, et al., 2002). Although the root system represents a critical evolutionary advantage for C_4 plants, it is not the only reason for their success. As mentioned above, atmospheric CO_2 is also an important factor. The low concentrations of this gas during the Pleistocene led to the expansion of C_4 plants, since they use a pump to transport CO_2

to their photosynthesis sites. Thus, under low CO_2 concentrations, phototranspiration allows C_4 plants to photosynthesize more effectively than C_3 plants. This would have favoured the spread of C_4 plants from equatorial regions during glaciations. At the beginning of the Holocene, there was a greater abundance of C_4 plants available in low-elevation ecosystems in America mid-latitudes (30°-40°) (MacFadden, et al., 1999, MacFadden, et al., 1996). This predominance appears to decline at the end of the early Holocene. Isotopic studies of carbonates formed on paleosoils from Chihuahuan desert in New Mexico, indicate that after 9,000 yr BP, but no later than 7,000 yr BP, there was a decrease of C_4 grasses and a replacement by C3 grasses and shrubs, due to an increase in atmospheric CO2 from ~ 180 ppmv (during the last glacial maximum, 18,000 yr BP) to ~ 275 ppmv at 10,000 yr BP. (Cole and Monger, 1994).

The Guanaco: diet and isotopic values

The guanaco is a wild ungulate widely distributed in South America, exhibiting a highly flexible behaviour as reflected in the alternation between grazing and browsing, as well as variations in their social organization (Puig and Videla, 1999, Wheeler, 1991). **This species inhabit steppes, shrub steppes**, and even wooded areas, and populations may be sedentary or show migratory movements (Franklin, 1983, Ortega and Franklin, 1995, Raedeke, 1979). In common with other South American camelids, the guanaco is adapted to forage consumption of low nutritional value, typical of arid ecosystems, which is achieved through improved digestive efficiency and a lower rate of intake than true ruminants (San Martín and Bryant, 1988). The diet consists mainly of grasses (61.5%), followed by small leaves and branches of trees and shrubs (15.4%), “clavel del viento” or “barba de Viejo” (*Pilosocereus alensis*) (6.9%), lichens (*Usena* spp.) (2.4%), fungi (2.6%), as well as herbs and several shrubs 11.2% (Raedeke, 1979). The grasses

consumed throughout the year are mainly composed of *Festuca gracillina* and *Festuca magellanicum*, but in March the diet changes significantly and becomes dominated by the branches of trees and shrubs (60%). In very similar landscapes to those surrounding the Traful I cave, communities are dominated by grasses (*Stipa speciosa* and *Festuca pallescens*) and shrubs (such as *Mulinum spinosum*), with small proportions of sub-Antarctic forest galleries along the rivers and canyons.

According to the faecal composition, the guanaco diet in spring is composed of forbs (44.3%), grasses (32.4%), trees and shrubs (13.8%) and plants (6.7%). The main foraged species are *Acaena* spp. (38%), *Festuca pallescens* (13.8%) and *Poa* spp. (9.9%). During the summer, 50% of the intake is represented by *Acaena* spp, 11.5% by *Poa* spp and 5.7%. by *Colletia spionosissima.* The summer diet contains less grass and plants than the spring diet. However, the overall yearly diet is mainly composed of trees and shrubs (59.6%), followed by herbs (15.4%), grasses (15.4%) and plants (5.6%), reflecting the higher intake of trees and shrubs during the autumn and winter than during the spring and summer (Bahamonde, et al., 1986). Similar results were obtained in the forest-steppe ecotone of Tierra del Fuego (Bonino and Sbriller, 1991).

Another study of guanaco diet based on faecal matter composition was undertaken in the La Payunia Reserve (Mendoza), a grassland landscape with isolated shrubs (Puig, et al., 1997, Puig, et al., 1996) and two differentiated environments characterized by their soil and vegetation. The first environment is dominated by sandy soils and grasses, while the second is characterized by a steppe with co-dominance of grasses and shrubs in a basaltic steppe landscape. In these environments, the guanacos show a preference for grasses and herbs over bushes in spring and summer, compared with the higher intake of shrubs and bushes during winter and autumn. In stony environments, the

predominant preferred species is *Stipa* sp, but the guanacos also consume *Poa* and *Panicum*, and their diet can be supplemented with large proportions of *Hyalis* (bush with little woody tissue). However, the authors (Puig, et al., 1997) point out that, when the availability of *Poa* decreases in winter, guanacos prefer *Hyalis* shrubs that are easily available in the rocky habitat. This fact reflects the continued stability of the guanaco in these environments throughout the year, while, in other environments, there is a migration in search for shelter and food. As mentioned above, these two studies of the guanaco diet were performed by the analysis of pellets of faecal matter. By contrast, a study based on direct observation (Candia and Dalmasso, 1995) shows that, out of a total of 65 plant species surveyed in the La Payunia Reserve, 47 (72.3%) are consumed throughout the year. Among the identified species, shrubs make up 66.7% of the diet, while the grasses account for 26.3%. The most consumed species is *Panicum urvelleanum*, a C_4 pathway plant (Cavagnaro, 1988).

From these studies, we can infer that there is a marked change in the diet of guanaco between spring-summer and autumn-winter. The low availability of grass in the colder months forces the animals to migrate in search of food and shelter. If we look at the entire year, the guanaco forages on trees and shrubs, followed by grasses. According to these authors (Bonino and Sbriller, 1991, Candia and Dalmasso, 1995, Puig, et al., 1997, Raedeke, 1979), the grasses only account for the majority of the diet in the summer months. We must take into account that these studies are based on current observations in environments with co-occurrence of domesticated animals (sheep, goats and cattle). Grazing studies have demonstrated the negative impact of these animals. Bertiller and Bisigato (1998) emphasize that the first effect of overgrazing by sheep herds in the sub Antarctic grass steppe zone is a decrease in the variety of available

grasses and a replacement of *Festuca pallescens* (grass) by *Mulinum spinosum or Senecio* spp. (bush), or, in the worst scenario, by dwarf shrubs of the genus *Acaena*. Other plants consumed by guanacos, such as *Aristida* sp. *Springfield il Bothriochloa*, *Panicum urvelleanum*, *Poa lanuginosa* and *Sporobolus rigens*, also exhibit a C_4 photosynthesis pathway (Llano, 2009, see Table 3, pp. 139).

Currently, there are not isotopic studies of guanaco's diet available, nor lipids or bulk. For a spatial and temporal trend of available isotopic data for guanaco see Barberena, et al., (2009) and Barberena, et al. (2010), (Barberena, et al., 2009).

A synthetic paleoenvironmental history of north-western Patagonia

Several authors claim that deglaciation started at between 14,000 and 13,000 yr BP, with a minor return towards cold climatic conditions called the "Huelmo-Marscardi cold reversal" between 11,400 and 10,200 yr BP (Ariztegui, et al., 1997, Bianchi, et al., 1999, Heusser, et al., 1996). This last degradation of climatic conditions corresponds to the Younger Dryas. However, for the beginning of the Holocene, several studies (pollen and charcoal sequences) have shown that the climate became drier and warmer (Denton, et al., 1999, Heusser, et al., 1996, Markgraf, 1983, Whitlock, et al., 2006).

In northwestern Patagonia, the pollen record of Mallín Book starts at around 13,000 BP. At that time, the pollen assemblage is characterized by Gramineae, herbaceous taxa and shrubs, with less than 10% of *Nothofagus* pollen, a C_3 specie (Read and Farquhar, 1991). This suggests that the steppe environment expanded considerably westward into the Andean valleys during late glacial times (Clark, et al., 2012, Cusminsky, et al., 2011, Markgraf, 1983, Markgraf, et al., 2013, Markgraf, et al., 2002, Markgraf, et al., 2009, Whitlock, et al., 2006). The moisture appears to have increased between 13,000 and 12,500 yr BP because the *Nothofagus* influx leads to relative abundances in excess

of 50% during this transitional period. By the end of the Pleistocene and early Holocene, open forest with substantial elements of grass-shrub steppe was already established in the foothills of the eastern Andes, (Markgraf, 1983, Whitlock, et al., 2006). The palynological analysis of soils from Epullán Grande cave indicates the existence of three zones: EG1, EG2 and EG3. The EG1 zone (Epullán Grande 1) (9,970-7,000 yr BP) indicates wetter conditions than today (Prieto and Stutz, 1996). The EG2 zone (7,000-5,140 yr BP) yields elements of the western steppe shrubs, suggesting the onset of the establishment of typical vegetation in this region, with environmental conditions similar to the present. Data from the Traful I cave, located in the forest-steppe ecotone of the sub-Andean district, show no significant climatic fluctuations during the early Holocene (Heusser, 1993), while the sequence of small mammals suggests that environments remained basically stable over some 9,400 years (Pearson and Pearson, 1993). However, Pardiñas and Teta (2008), Pardiñas and Teta (In press) highlight the lack of *Geoxus valdivianus*, *Irenomys tarsalis* and *Oligoryzomys longicaudatus* along with the low abundance of *Octodon bridgesii* and the high abundance of *Abrothrix olivaceus* in layers 20 to 18 of Traful I cave. These features indicate a landscape composed of more open environments than today, where patches of forest would be reduced under colder and probably drier conditions. In layers 16 and 17, the emergence of other rodents such as *Geoxus valdivianus*, *Irenomys tarsalis* and *Oligoryzomys longicaudatus* are clear indications of more humid conditions and increased tree cover around Traful I during this period (Pardiñas and Teta, In press). By the end of the early Holocene and the beginning of the middle Holocene (layers 15 to 10 and layers 9 to 7), we can note a small change associated with the emergence of *Eligmodontia* spp. and *Galea leucobephara*. Both species are representative of steppe

environments and reflect the development of arid conditions. Consequently, the relative abundance of *Abrothrix longipillis* reaches the lowest value obtained in this record. During the late Holocene, after the deposition of volcanic ash, two species are recorded (*Phyllotys xanthopygus* and *Reithrodon auritus*) which then show an increase in their abundance. The occurrence of these species, together with *Lestodelphis halli* - a typical marsupial of West-Central Patagonia - points to the existence of open steppe and extensive bare rock (Pardiñas and Teta, 2008, Teta pers. comm.).

The continuous presence of pollen derived from the steppe at 7,000 yr BP indicates that the evergreen *Nothofagus* forest remained open (Markgraf, et al., 2013). Between 7,000 and 5,000 yr BP, the climate became drier (more continental) with cold winters. From 5,000 until 3,000 yr BP, tree pollen increases to 90% of the total. The pollen record of EG3 from Epullán Grande cave (5,000-1,720 yr BP) shows that the vegetation communities of Western Patagonia would have been locally established from 5,000 yr BP onwards. The pollen association and its relative abundances are similar to those observed in the transition between the *Mulinum* shrub-steppe (in the west) and the Monte formation (in the east) (Prieto and Stutz, 1996, Stutz, 1994).

From 3,000 yr BP onwards, the abundance of pollen from the steppe substantially increases suggesting a decrease in precipitation. With the exception of a brief return of forest around 2,000 yr BP, the open forest conditions continued until the recent past (Markgraf 1983:56). Studies of the age structure of trees and similarities of photographs show an expansion of the steppe and forest, with a dominance of shrubs in the steppe over the last few centuries. Changes first occurred during the 14th century following the cessation of occasional intentional fires caused by indigenous groups, with the subsequent expansion of shrubs being mainly due to overgrazing of sheep since the

beginning of the 20th century (Veblen and Lorenz, 1988). For a photosynthetic pathway and some isotopic values of the pollen taxa consult Llano (2009, see Table 3, pp. 139).

3. Materials and methods

To infer the values of $\delta^{13}C$ values of fatty acids in bones and soils, we selected 14 bones of guanaco (*Lama guanicoe*) from each layer of Traful I cave and the most ancient occupations one from LL (Epullán Grande, strata 07). It appears that all the layers yield bones that can be unequivocally assigned to this taxon (Cordero, 2009, Cordero, 2011a, Cordero, 2011b). As a result, we can obtain a consistent sequence that extends from layer 15 to the final occupations.

We follow the protocol adopted by Lucquin and March (2003), March (1995), March (1999), March and Lucquin (2006) for fatty acid extraction. And also we take into account others authors like DeNiro and Epstein (1977), Evershed, et al. (1995), Jim, et al. (2004), Stott, et al. (1997). The bones were washed with deionized water and cleaned with methanol by ultra-sonication for 90 min. to clean all contamination in the surface. An extensive drilling was not necessary. After that, the samples – 120 grs in the case of sediments and, for the bones see Table 1– were extracted twice, according to each volume, with a chloroform (300 ml) /methanol (150 ml) solution (2:1) by ultra-sonication for 90 min. at 40°C. The solution so obtained was then separated by the method of McCarthy and Duthie (1962) using a chromatographic column of silica gel impregnated in potassium hydroxide (10 g). The neutral compounds were first eluted with ethyl ether (100 ml). The fatty acid compounds were eluted with 2% formic acid in ether (100 ml), and then transformed into their corresponding methyl ester by treatment with a solution of acetyl chloride in methanol for 20 min at 80 °C. The acid fraction

were then analysed by GC (gas chromatography) and gas chromatography coupled with mass spectrometry (GC/MS). Compounds were identified by their retention time within the GC, their fragmentation pattern within the MS and by matching their mass spectra with reference spectra from the literature or from libraries (NBS75K and Wiley). Finally, we performed GC-C-IRMS of methylated saturated fatty acids ($C_{16:0}$ and $C_{18:0}$) from each layer and bone sample. To determine the state of conservation of the organic matter we will use the Preference Carbon Index (CPI), according to Cooper and Bray (1963) the formula is:

$$\text{CPI (fatty acids)} = \frac{1}{2}\left[\frac{\sum_{21}^{n} \text{even chains}}{\sum_{20}^{n-1} \text{odd chains}} + \frac{\sum_{21}^{n} \text{even}}{\sum_{22}^{n+1} \text{odd}}\right]$$

GC analysis

The GC analyses were carried out with a Hewlett Packard (HP 6890 series) instrument equipped with a FID detector at a temperature of 250°C, using a HP-5 capillary column with 5% phenyl methylpolysiloxane polymer, 0.25 mm internal diameter, 30 m length and 0.25 mm phase thickness. Helium was used as carrier gas (1 ml/min flow rate). The injector was in splitless mode and maintained at 250°C. The oven temperature was ramped from 40 to 300°C at 4 °C/min and held for 30 min at 300 °C.

GC-MS analysis

The GC/MS analyses were performed with a Hewlett Packard instrument (HP 6890 coupled to an HP 5973 quadrupole mass selective detector) equipped with a DB-ms non-polar capillary column, using 5% Phenyl Methylpolysiloxane polymer, 0.25 mm internal diameter, 30 m length and 0.25 mm phase thickness. The chromatography was carried out under the same conditions as for GC analysis. The MS was operated in

electron impact mode at 70 eV, using a source temperature of 250 °C, an emission current of 1 mA and multiple-ion detection with a mass range from 40 to 800 amu.4.

GC-C-IRMS measurements:

The carbon-13 content of palmitic ($C_{16:0}$) and stearic ($C_{18:0}$) acids in the form of fatty acid methyl esters (FAME) was determined by gas-chromatography-combustion-isotope ratio mass spectrometry (GC-C-IRMS), either on a Carlo Erba GC 8130 chromatograph interfaced with a VG Isochrom mass spectrometer (Fisons Instruments, Altrincham, England), or on a HP6890N instrument (Agilent technologies, Hewlett Packard) interfaced with an Isoprime mass spectrometer (GV Instrument, Manchester, UK). These analyses were performed at the UMR 1348 Pegase laboratory by Jean Noel Thibault and Philippe Ganier.

Briefly, the effluent stream from the capillary GC column enters a combustion furnace where compounds are quantitatively combusted to CO_2 and water. Water is then removed from the carrier stream using a cryogenic trap, and the sample-derived CO2 is then analysed by high-precision IRMS for its carbon-13 content. In both systems, temperatures in the interface and combustion oven are regulated to 350°C and 850 °C, respectively, and the carrier gas (He) is introduced at a constant flow rate of 1.2 ml/min.

Separation of fatty acid methyl esters was performed on a DB-5MS capillary column (J&W Scientific, Courtaboeuf, France) with the following characteristics: 30 m, 0.25 mm i.d. and 0.25 µm film thickness. Depending on their FAME concentrations, samples were injected either in split or in splitless mode and analysed at least in duplicate.

In this study, the optimal chromatographic conditions were as follows: with an injector temperature of 240°C, the column was held isothermal at 45°C for 2 min after injection.

The temperature was first increased at a rate of 8°C/min up to 180°C, then at 3°C/min up to 205°C and finally at 20°C/min to 300°C, where it was held for 2 min.

The stable carbon isotopic composition is reported using the conventional delta per mil notation ($\delta^{13}C$), expressed relative to the international Vienna Pee Dee Belemnite standard (V-PDB), according to the following equation:

$$\delta^{13}C\ ‰ = \left[\left(\frac{^{13}C}{^{12}C} \right)_{sample} / \left(\frac{^{13}C}{^{12}C} \right)_{PDB} - 1 \right] \times 10^3$$

The calibration is performed using a bottle of reference CO_2 connected to the IRMS system, which introduces three pulses directly into the source at the beginning and end of every isotopic GC determination and 5 pulses during acquisition of the chromatogram to take account of potential background changes during the run. Analyses were all performed using IonVantage software for Isoprime (build 1.3.6.0); Accuracy and precision on reference gas pulses in each run were better than 0.3‰, which corresponds to the specification of the system. The carbon-13 content of the reference CO_2 was previously calculated by means of an inter-laboratory comparison study using 6 different standards analysed in 20 laboratories either with EA-IRMS or GC-C-IRMS systems.

The $\delta^{13}C$ values of FAME were corrected to take account of the dilution of fatty acid carbon by the methylating reagent. This isotopic shift was calculated by a mass balance equation:

$$\delta^{13}C_{FAME} = f_{FA}\delta^{13}C_{FA} + f_{MeOH}\,\delta^{13}C_{MeOH}$$

where $\delta^{13}C_{FAME}$, $\delta^{13}C_{FA}$ and $\delta^{13}C_{MeOH}$ are the carbon isotope compositions of the fatty acid methyl ester, the fatty acid, and the methanol used for methylation of the fatty acid, respectively, while fFA and fMeOH are the carbon fractions in the fatty acid methyl ester due to the alkanoic chain and methanol, respectively. In this case, the f_{FA} values is 16/17 for $C_{16:0}$ and 18/19 for $C_{18:0}$. The carbon-13 content of methanol was analysed by EA-IRMS (CA1500 NC Elementary Analyzer, Carlo Erba, Milano, Italy / Isoprime isotopic ratio mass spectrometer, GV Instrument, Manchester, UK), yielding δ^{13}CMeOH = - 40,5‰ (n=5, SD=0.3‰).

Finally, the day-to-day and long term analytical accuracy of the 2 GC-C-IRMS systems were checked by the injection of an in-house mixture of FAMEs ("FAMEs from cattle grilled on a hot stone") in each analysis batch: the $\delta^{13}C$ values for $C_{16:0}$ and $C_{18:0}$ are respectively -28.48‰ (SD=0.37‰) and -30.33 ‰ (SD=0.37‰) for 18 analyses within one year.

4. Results

We obtained 21 isotopic values of $\delta^{13}C_{16:0}$ and $C_{18:0}$ from the acid fractions of fatty acid (Table 1 and Figure 4). We choose use these fractions because they are the most abundant in the sample and we are sure about their origin, and reporting the presence of other fatty acids helps to determine the source of the carbon. The carbon preference index (CPI) of fatty acids is well preserved, since only the soil in layer 12 (CPI < 3) and bone material in layer 10 (5.55) have low values that indicate a relatively poor conservation (Table 1). Even though the CPI of layer 10 indicates a moderate degree of conservation, this is unrelated to the amount of FAME recovered (Table 3), which is the maximum observed in all the samples.

By comparing the $\delta^{13}C_{16:0}$ and $\delta^{13}C_{18:0}$ values of fatty acids with the bulk data obtained by other researchers (Barberena, et al., 2010, Barberena, et al., 2009) we can see that our results show more negative values. We should take into account the fact that the isotope values of $\delta^{13}C$ on bone fat are naturally lower than those of collagen (Howland, et al., 2003), like in grassland studies (Dungait, et al., 2008, Dungait, et al., 2010, Dungait, et al., 2011). We also note that the $\delta^{13}C_{18:0}$ values show less variability and have an outlier (Layer 15 = -22.25‰, Table 1). The values of $\delta^{13}C_{16:0}$ show more variability, but not outliers. The only outlier observed (layer 15) cannot be explained in terms of FAME mass or conservation (CPI). There is a significant and strong correlation (Table 3) between the sample mass and the extracted amount of $C_{18:0}$ FAME, but the correlation with $C_{16:0}$ is very weak, indicating an increase in mass that could reflect a relation between the amount of fat and its conservation (Table 3). Other correlations are non-significant, showing that the variables are independent and that the isotope values are influenced by the change in guanaco diet over time.

This bones fatty acid could have come from the soil or, in the worst case scenario; could have been contaminated by soil? Evershed, et al. (1995: 290) stressed that "The presence of lipids in ancient bones with compositions and structures that are markedly different to those that are seen in soil extracts indicates that the lipids in bone are not derived from the soil by migration of diffusion." A solution is reporting the presence of other fatty acids, especially branched and triacylglycerols, as well as cholesterol, might help to determine the source of the carbon, and hence, would also help with the interpretation of the carbon isotope data. They might, for example, show that the bone lipids are, in fact, authentic to the camelids (and unlike to the expected for bacteria or lipids from human fingers handling the bone). If we compare the extracted soil and the

bones (Table 2) we find that in the soils samples there are branched chain fatty acid and different kinds of unsatured fatty acids, like $C_{16:1}$, $_{C18:1}$ and $C_{18:2}$, that are not present in the bones samples. The only exceptions are layer 4 and 14, were we have $C_{16:1\omega9}$ (layer 4), $C_{16:1\omega7}$ (layer 14) and $C_{18:1\omega10}$ in both of them. The contamination that we could find, only in the soils, was 13-Docosenamide, (Z)- (see Table 2) that came from the plastics bags where they were stored for 30 years. Then the obtained bones values were not contaminated by the fatty acid nor from the soil neither from human fingers and also not the result of bacterial activities.

As we can see in Table 1, the values of $\delta^{13}C_{16:0}$ and $\delta^{13}C_{18:0}$ fluctuate throughout time. Such variations can be prompted by the changing intake of C_3/C_4 plants available in local or regional environments. According to Copley, et al. (2003), Copley, et al. (2005), Evershed, et al. (2008), Gregg, et al. (2009) and March (In press), the individual $\delta^{13}C_{16:0}$ and $\delta^{13}C_{18:0}$ fatty acid signatures are enriched following an increment in the intake of C_4 plants. Figure 6b (ΔC13 / $\delta^{13}C_{16:0}$) shows the limit value of -26‰ $\delta^{13}C_{16:0}$ ($^0/_{00}$) for discriminating C_3 from C_4 diet as proposed by Evershed (2008) following Copley, et al. (2003), Copley, et al. (2005). This analysis reveals two groups, one associated with a predominantly C_3 diet and the other showing values typical of an increasing C_4 diet. Therefore, a large proportion of our samples show $\delta^{13}C_{16:0}$ and $\delta^{13}C_{18:0}$ enrichment at different episodes during the Holocene that can be attributed to increases in C_4 plant intake. Based on the bone analyses, these increases took place during deposition of layers 15, 8, 6 and 4 (Table 1). The values of $\delta^{13}C_{16:0}$ and $\delta^{13}C_{18:0}$ in soils follow the same fluctuation trend. As with the bones, two different groups of samples can be recognized based on analysis of soils. Soils could be expected to have a less enriched signature than bones (Eglinton and Eglinton, 2008, Jacob, et al., 2007), so

we can assume that the same phenomenon of enrichment occurs in both kinds of samples, but with a small shift. Moreover, the increase in C_4 diet sometimes occurs at much lower values as found by Gregg, et al. (2009, see Fig. 5), who propose a discriminant threshold of -30‰ $\delta^{13}C_{18:0}$. These authors plot $\delta^{13}{}_{C18:0}$ on the X axis. In any case, the enrichment of $\delta^{13}C$ values is produced by the same phenomenon. However, before interpreting these results, we need to discuss some concepts concerning the isotopic C cycle and its relation with guanaco diet.

5. Discussion

Biosynthetic pathways should be reflected by the $\delta^{13}C$ signature of individual fatty acids in guanaco bones, so these values could be a good indicator of diet fluctuations due to modifications in vegetation intake. Our $\delta^{13}C$ values of the fatty acid methyl esters (FAMEs) of $C_{16:0}$ and $C_{18:0}$ from guanaco bones can be correlated with other proxies available for the region, such as palynological data from Moreno Lake (Figure 4) and Cordón Serrucho Norte (Figure 5) (Markgraf, et al., 2013, Markgraf, et al., 2002). Other behavioural factors (population size, migration patterns, sex and age differences within a guanaco population) that could influence all the stable isotope animal signatures are not studied yet and then cannot be taken into account for this article.

Early Holocene

During this period, the forest-steppe ecotone transition was already established (Markgraf 1983:54). With the increase in available moisture, from 13,000 to 12,500 yr BP, the *Nothofagus* forest extended eastward, although the continued presence of steppe-derived pollen up to 7,000 yr BP suggests that the forest remained open (Markgraf, et al., 2013, Markgraf, et al., 2002). Pardiñas and Teta (2008), Pardiñas and

Teta (In press) also suggest that the environments were more open than today, with reduced forest patches under colder and probably drier conditions.

According to soil isotopic signal (Table 1) of layer 21 ($C_{16:0}$ = -27.08‰ - $C_{18:0}$ = -27.63‰), this value is close to the bone from #07 of Epullán Grande ($C_{16:0}$ = -26.07‰ - $C_{18:0}$ = -27.70‰), 86 km east way. We could assume that both, the bone (from LL cave) and the sediments (from Traful I) are linked. We assume that both caves share the same isotopic ambient and there is a link between the sediments and the bones in the early and middle Holocene values. In the case of the Traful I sequence this connection is significant. The R Pearson = 0.87 p>0.05 for the layer 21 to 10, and 0.03 p>0.05 for the all sequence.

The presence of a *Myocastor coypus* jaw in layer 16, a semiaquatic rodent (Cordero, 2011a), together with *Geoxus valdivianus*, *Irenomys tarsalis* and *Oligoryzomys longicaudatus* in the sterile layers (17 and 16) are clear signs of more humid conditions around Traful I, as pointed out by Pardiñas and Teta (In press). The isotopic values of layer 15, formed after 9,000 BP., show an increasing C_4 diet, a period coinciding with the predominance of these plants reported by Cole and Monger (1994). Also, according to current studies in central Argentina, C_4 grasses dominate in terms of number of species at the elevation of the Traful I cave (situated at 760 m above sea level), but not in coverage, which is equilibrated with C_3 plants (Cabido, et al., 1997, Cavagnaro, 1988). This could either indicate that C_4 plants are now dominant in the landscape or, despite the equilibration of coverage between C_3 and C_4 plants, the guanaco currently prefers C_4 plants (like *Panicum urvelleanum* o *Sporobolus rigens*, for example). We should note that, at the end of the early Holocene, the pollen record indicates an increased tree cover in the vicinity of the cave (Heusser, 1993). Therefore, we propose

that the guanaco remains in layer 15 were deposited when the forest remained open with a high grasses coverture near Traful I and the predominant diet of these ungulates was based on C_4 plants (Figure 3b).

Middle Holocene

A radical shift in guanaco diet takes place towards a predominance of C_3 plants and is clearly observed in the transition from layer 15 to 13 (Figure 4 and Figure **5**). This period corresponds to the onset of a more arid environment around 8,000 yr BP, as recorded in several regions of South America (Gil, et al., 2005, Markgraf, et al., 2003, Markgraf, et al., 2009, Moreno, 2004, Stine and Stine, 1990). We see a shift to an environment dominated by shrubs rather than grasses (Figure **3**c). This process coincides with the deposition of layer 13 (7,855 ± 70 and 7,308 ± 285 yr BP), when the guanaco diet may have been based mainly on C_3 plants. Shrubs are better adapted to drought than grasses because they have deep roots that can use the remaining moisture in the layers farther from the surface (Aguilar and Sala, 1998). Thus, considering that the guanaco diet is predominantly based on trees and shrubs (as has been pointed by Bonino and Sbriller, 1991), the development of shrub vegetation may correlate with the C_3 signature (Figure 3c). Several authors (Abarzúa, et al., 2004, Lamy, et al., 2001, Markgraf, et al., 2009, Moreno, 1997, Veit, 1996) claim that a change in the activity of westerlies (latitudinal displacement/strength) around 8,000 years ago had a major impact on the precipitation pattern with, for example, Laguna Aculeo showing desiccation between 8,400 and 5,000 ^{14}C yr B.P. (Jenny, et al., 2002). These features are compatible with the palaeoenviromental reconstruction of temperature and precipitation proposed by Heusser and Streeter (1980, see Fig. 2). All these data indicate that the change in guanaco food intake can be strongly correlated with this climatic change and

correlated with the pollen data from Moreno Lake (Figure 4) and Cordón Serrucho Norte (Figure 5).

During the accumulation of layers 12 to 10, we can infer there was a relatively stability in guanaco feeding behaviour (Figure 4 and Figure 5). This episode is characterized by an increase in C_4 plants in view of the low $\delta^{13}C$ values recorded in the underlying layer 13. The increase of $\delta^{13}C$ is accentuated between layers 10 and 8, where guanaco diet appears to reflect a greater intake of C_4 plants but does not reach the values observed in layer 15. The entire process leading to an increase in C_4 plants takes place over an interval of about 1,000 years. During this interval, the mean annual precipitation in Chile increases, and this trend continues up until 4,950 ± 400 yr BP (Heusser and Streeter, 1980). By 6,000 yr BP, the prevailing environmental conditions are cool with a progressive increase in precipitation (Mancini, et al., 2005, Markgraf, 1983). During this period, there is a new development of the forest on ecotonal zones with increased availability of pasture (Markgraf, et al., 2013). Unfortunately, there are no data on bones from layer 7, but soils shows a decline in $\delta^{13}C$ values, with an increasing C_3 signature that attains its maximum in layer 6.

Between 5,000 and 3,000 yr BP, there is an increase of moisture in a climate that becomes colder compared with the previous period (Heusser and Streeter, 1980). During this interval, there are no occupations in Traful I cave. The guanaco bone analysed in this layer yields a relatively enriched C_4 signature, showing no significant difference from values observed in layer 8. Similar values are observed in layer 4, while sediments reflect a rapid increase in C_4 plants. Therefore, the fluctuations observed in soil samples are not actually reflected in the analysed bones from the same layer.

Late Holocene

During the late Holocene, there is a new development of forest and the ecotone shifts to the east due to an increase in rainfall between 2,700 and 2,200 yr BP (Figure 3d). The guanaco diet varies and the carbon isotope signature increases to the values attained in the layers 8 to 4, but then decreases in the tephra layer and level 3 (Figure 4). This tephra event was dated recently between 1,950-2,500 cal. yr BP, which overlaps with the result obtained for Layer 3A of Traful I (Villarosa, et al., 2006). While we observe a volcanic ash layer in the sediment sequence, it is also important to mention that the tephra event has a clear isotopic signature that is associated with a marked progression of C_3 plants. The soils of layers 3 and 2 show a renewed enrichment of the $\delta^{13}C$ signature.

For this latest period of development of the forest, there are an "increased proportion of *Nothofagus dombeyi* type that suggests the tree was actually growing in the region" (Mancini, et al., 2005). The vegetal signature became more strongly marked in layer 4, with an increase of vegetal biomarkers, long chain alkanes and sterols, which then drop progressively in layers 3 and 2 when human impact returns (Cordero, 2011a). These three topmost layers match with a nearby *Astrocedrus* forest environment. Above layer 2, we have no further information, and we must refer to the most reliable source of paleoenvironmental data (Villalba, 1990, Villalba, 1994).

Some human implications of this study

Even if the forest not reached Traful I at the end of early Holocene (Layer 15 or earlier), it is possible that the guanaco population were not present or had low densities. Hunter-gatherers would have been conditioned by this fact. The isotopic values of layer 13 could be interpreted as indicating a dry period in the vicinity, and therefore, a greater

abundance of guanacos in this area. In this context, the guanaco begins to be more abundant and is established as the main food resource at the end of middle Holocene in the forest-steppe ecotone. However, the exploitation of small game remains significant. The beginning of Component I at Traful is accompanied by a change in the prior lifestyle (Cordero, 2012, Crivelli Montero, 2011). The hunter-gatherers who occupied the cave during this period were users of a different lithic technology.

6. Conclusions

This study explored the use of $\delta^{13}C$ analysed in individual fatty acids extracted from bones which, in some cases, can help to reconstruct animal diet and, as a consequence, the paleoenvironments of archaeological sites. We also show that the $\delta^{13}C$ values in individual fatty acids of soils follow the same trend observed in bone materials (Layer 21 to 10), and are a valuable paleoclimatic biomarkers. The observed variation seems to be related to changes in climate and vegetation, implying a displacement of the ecotone around Traful I. This displacement of the forest-steppe ecotone can explain some hunter-gatherer behaviours. In this way, $\delta^{13}C$ values of fatty acids from guanaco bones follow other proxy like pollen columns and could be relevant in reconstruct ancient environments. With further calibration of the radiocarbon dating and stable carbon isotope signatures, it would be possible to interpret local paleoenvironmental sequences. Such an approach could provide a good illustration, for example, of the changes that occurred during the Little Ice Age and Medieval climate optimum, which are not recorded in the sequence studied here. In addition, we need to determine the accurate season of death of the guanacos in order to remove the effect of interannual isotopic variations due the summer-winter diet change. Therefore, due to the absence of entire

jaws, we will need to analyse the growth lines of dispersed teeth to determine the age of the guanacos.

Finally, we consider there is a need for more detailed studies on the relation between seasonal and long-term intake of C_3 and C_4 plants and the $\delta^{13}C$ of individual fatty acids in bones. For future studies, we aim to increase the number of samples in each layer and thus enhance the amount of data obtained. Moreover, these studies should improve the potential of this method to reconstruct past animal behaviours and their eventual impact on human subsistence.

Acknowledgements

We are especially grateful to Eduardo A. Crivelli Montero for providing the opportunity to carry out this work. The project was funded by the Argentine National Council of Science CONICET (PIP 112-200801- 01605), the Agency of Science FONCyT (PICT 14.171), the University of Buenos Aires (UBACyT 20020100100266), and a research grant awarded by the French Embassy in Argentina and the French Ministry of Education.

The authors wish to thank J. N. Thibault and Ph. Ganier (Plateau Technique de Spectrométrie de Masse Isotopique INRA, UMR1348 Pegase, 35590 Saint-Gilles, France) as well as the OSUR-RENNES, for their collaboration in isotopic analysis.

References

Abarzúa, A.M., Villagrán, C., Moreno, P.I., 2004. Deglacial and postglacial climate history in east-central Isla Grande de Chiloé, southern Chile (43°S), Quaternary Research 62, 49-59.

Aceituno, P., 1988. On the Functioning of the Southern Oscillation in the South American Sector. Part I: Surface Climate, Monthly Weather Review 116, 505-524.

Aceituno, P., 1989. On the Functioning of the Southern Oscillation in the South American Sector. Part II. Upper-Air Circulation, Journal of Climate 2, 341-355.

Aguilar, R.A., Sala, O.E., 1998. Interaction among grasses, shrubs, and herbivores in Patagonian grass-shrub steppes, Ecología Austral 8, 201-210.

Ariztegui, D., Bianchi, M.M., Massaferro, J., Lafargue, E., Niessen, F., 1997. Interhemisferic synchrony of Late-glacial climatic inestability as recorded in proglacial Lake Mascardi, Argentina, Journal of Quaternary Science 12, 333-338.

Bahamonde, N., Martin, S., Sbriller, A.P., 1986. Diet of Guanaco and Red Deer In Neuquen Province, Argentina, Journal of Range Management 39, 22-24.

Balasse, M., Ambrose, S.H., Smith, A.B., Price, T.D., 2002. The Seasonal Mobility Model for Prehistoric Herders in the South-western Cape of South Africa Assessed by Isotopic Analysis of Sheep Tooth Enamel, Journal of Archaeological Science 29, 917-932.

Balasse, M., Bocherens, H., Mariotti, A., Ambrose, S.H., 2001. Detection of Dietary Changes by Intra-tooth Carbon and Nitrogen Isotopic Analysis: An Experimental Study of Dentine Collagen of Cattle (Bos taurus), Journal of Archaeological Science 28, 235-245.

Balasse, M., Smith, A.B., Ambrose, S.H., Leigh, S.R., 2003. Determining Sheep Birth Seasonality by Analysis of Tooth Enamel Oxygen Isotope Ratios: The Late Stone Age Site of Kasteelberg (South Africa), Journal of Archaeological Science 30, 205-215.

Barberena, R., Gil, A.F., Neme, G.A., Zangrando, F.A., Politis, G.G., Borrero, L.A., Martínez, G.A., 2010. Ecología isotópica de guanaco (*Lama guanaicoe*) en el sur de Sudamérica: tendencia espaciales, temporales e implicancias arqueológicas, in: Gutiérrez, M.A., De Nigris, M.E., Fernández, P.M., Giardina, M., Gil, A.F., Izeta, A.D., Neme, G.A., Yacobaccio, H.D. (Eds.), Zooarqueología a principios del siglo XXI. Aportes teóricos, metodológicos y casos de estudio, Ediciones del Espinillo, Buenos Aires, pp. 107-117.

Barberena, R., Zangrando, F.A., Gil, A.F., Martínez, G.A., Politis, G.G., Borrero, L.A., Neme, G.A., 2009. Guanaco (*Lama guanicoe*) isotopic ecology in southern South America: spatial and temporal tendencies, and archaeological implications, Journal of Archaeological Science 36, 2666-2675.

Bertiller, M.B., Bisigato, A., 1998. Vegetation dynamics under grazing disturbance. The state-and-transition model for the Patagonian steppes, Ecología Austral 8, 191-199.

Bianchi, M.M., Massaferro, J., Roman Ross, G., Amos, A.J., Lami, A., 1999. Late Pleistocene and early Holocene ecological response of Lake El Trébol (Patagonia, Argentina) to environmental changes, Journal of Paleolimnology 22, 137-148.

Bonino, N., Sbriller, A.P., 1991. Composición botánica de la dieta del guanaco (*Lama guanicoe*) en dos ambientes contrastantes de Tierra del Fuego, Argentina, Ecología Austral 1, 97-102.

Boschin, M.T., Maier, M.S., Massaferro, G.I., 2011. Une lecture pluridisciplinaire des analyses chimiques et minéralogiques de peintures rupestres de la Patagonie argentine, L'Anthropologie 115, 360-383.

Boschín, M.T., Seldes, A.M., Maier, M., Casamiquela, R.M., Ledesma, R.E., Abad, G.E., 2002. Análisis de las fracciones inorgánica y orgánica de pinturas rupestres y pastas de sitios arqueológicos de la Patagonia Septentrional Argentina, Zephyrus 55, 183-198.

Cabido, M., Ateca, N., Astegiano, M.E., Anton, A.M., 1997. Distribution of C3 and C4 Grasses Along an Altitudinal Gradient in Central Argentina, Jounal of Biogeography 24, 197-204.

Candia, R., Dalmasso, A.D., 1995. Dieta del guanaco (*Lama guanicoe*) y productividad del pastizal en la reserva de la Payunia, Mendoza (Argentina), Multequina 4, 5-15.

Cavagnaro, J.B., 1988. Distribution of C3 and C4 Grasses at Different Altitudes in a Temperate Arid Region of Argentina, Oecologia 76, 273-277.
Clark, P.U., Shakun, J.D., Baker, P.A., Bartlein, P.J., Brewer, S., Brook, E., Carlson, A.E., Cheng, H., Kaufman, D.S., Liu, Z., Marchitto, T.M., Mix, A.C., Morrill, C., Otto-Bliesner, B.L., Pahnke, K., Russell, J.M., Whitlock, C., Adkins, J.F., Blois, J.L., Clark, J., Colman, S.M., Curry, W.B., Flower, B.P., He, F., Johnson, T.C., Lynch-Stieglitz, J., Markgraf, V., McManus, J., Mitrovica, J.X., Moreno, P.I., Williams, J.W., 2012. Global climate evolution during the last deglaciation, Proceedings of the National Academy of Sciences 109, E1134-E1142.
Cole, D.R., Monger, C.H., 1994. Influence of atmospheric CO_2 on the decline of C4 plants during the last deglaciation, Nature 368, 533-536.
Cooper, J.E., Bray, E.E., 1963. A postulated role of fatty acids in petroleum formation, Geochimica et Cosmochimica Acta 27, 1113-1127.
Copley, M.S., Berstan, R., Dudd, S.N., Docherty, G., Mukherjee, A.J., Straker, V., Payne, S., Evershed, R.P., 2003. Direct Chemical Evidence for Widespread Dairying in Prehistoric Britain, Proceedings of the National Academy of Sciences of the United States of America 100, 1524-1529.
Copley, M.S., Berstan, R., Mukherjee, A.J., Dudd, S.N., Straker, V., Payne, S., Evershed, R.P., 2005. Dairying in antiquity. III. Evidence from absorbed lipid residues dating to the British Neolithic, Journal of Archaeological Science 32, 523-546.
Cordero, J.A., 2009. Arqueofauna de las primeras ocupaciones de cueva Epullán Grande, Cuadernos de Antropología 5, 159-188.
Cordero, J.A., 2011a. Arqueofauna de las ocupaciones tempranas de cueva Traful I, provincia del Neuquén, Argentina, Arqueología 17, 161-194.
Cordero, J.A., 2011b. Subsistencia y movilidad de los cazadores-recolectores que ocuparon cueva Traful I durante el Holoceno medio y tardío, Comechingonia virtual V, 158-202.
Cordero, J.A., 2012. Las prácticas de subsistencia de las sociedades cazadoras-recolectoras del noroeste de la Patagonia argentina a lo largo del Holoceno, Archaeofauna 21, 99-118.
Crivelli Montero, E.A., 2011. Dos economías y dos tecnologías en el período antiguo de la prehistoria de la cuenca del Río Limay, in: Laferrère, C.M., Rivero, F., Díaz, J. (Eds.), Arqueología y etnohistoria del centro-oeste argentino, Universidad Nacional de Río Cuarto, Río cuarto, pp. 17-25.
Crivelli Montero, E.A., Curzio, D., Silveira, M.J., 1993. La estratigrafía de la Cueva Traful I (provincia del Neuquén), Præhistoria 1, 9-160.
Crivelli Montero, E.A., Pardiñas, U.F.J., Fernández, M.M., Bogazzi, M., Chauvin, A., Fernández, V.M., Lezcano, M.J., 1996. La Cueva Epullán Grande (provincia del Neuquén, Argentina). Informe de avance, Præhistoria 2, 185-265.
Cusminsky, G., Schwalb, A., PÉRez, A.P., Pineda, D., Viehberg, F., Whatley, R., Markgraf, V., Gilli, A., Ariztegui, D., Anselmetti, F.S., 2011. Late quaternary environmental changes in Patagonia as inferred from lacustrine fossil and extant ostracods, Biological Journal of the Linnean Society 103, 397-408.
Chan, Y.L., Hadly, E.A., 2011. Genetics variation over 10 000 years in *Ctenomys*: comparative phylochronology provides a temporal perspective on rarity, envoromental change and demography, Molecular Ecology 20, 4592-4605.
Chan, Y.L., Lacey, E.A., Pearson, O.P., Hadly, E.A., 2005. Ancient DNA reveals Holocene loss of genetic diversity in a South American rodent, Biology letters 1, 423-426.
DeNiro, M.J., Epstein, S., 1977. Mechanism of Carbon Isotope Fractionation Associated with Lipid Synthesis, Science 197, 261-263.
Denton, G.H., Lowell, T.V., Heusser, C.J., Moreno, P.I., Andersen, B.G., Heusser, L.E., Schlüchter, C., Marchant, D.R., 1999. Interhemispheric Linkage of Paleoclimate during the Last Glaciation, Geografiska Annaler. Series A, Physical Geography 81, 107-153.
Duan, Y., Wen, Q., Zheng, G., Luo, B., Ma, L., 1997. Isotopic composition and probable origin of individual fatty acids in modern sediments from Ruoergai Marsh and N ansha Sea, China, Organic Geochemistry 27, 583-589.

Dungait, J.A.J., Docherty, G., Straker, V., Evershed, R.P., 2008. Interspecific variation in bulk tissue, fatty acid and monosaccharide δ13C values of leaves from a mesotrophic grassland plant community, Phytochemistry 69, 2041-2051.
Dungait, J.A.J., Docherty, G., Straker, V., Evershed, R.P., 2010. Seasonal variations in bulk tissue, fatty acid and monosaccharide δ13C values of leaves from mesotrophic grassland plant communities under different grazing managements, Phytochemistry 71, 415-428.
Dungait, J.A.J., Docherty, G., Straker, V., Evershed, R.P., 2011. Variation in bulk tissue, fatty acid and monosaccharide δ13C values between autotrophic and heterotrophic plant organs, Phytochemistry 72, 2130-2138.
Eglinton, T.I., Eglinton, G., 2008. Molecular proxies for paleoclimatology, Earth and Planetary Science Letters 275, 1-16.
Ehleringer, J.R., Cerling, T.E., Hellinker, B.R., 1997. C4 photosynthesis, atmospheric CO2, and climate, Oecologia 112, 285-299.
Evans, C.J., Evershed, R.P., Black, H., Ineson, P., 2003. Compound-Specific Stable Isotope Analysis of Soil Mesofauna Using Thermally Assisted Hydrolysis and Methylation for Ecological Investigations, Analytical Chemistry 75, 6056-6062.
Evershed, R.P., 2008. Experimental approaches to the interpretation of absorbed organic residues in archaeological ceramics, World Archaeology 40, 26-47.
Evershed, R.P., Dudd, S.N., Copley, M.S., Mutherjee, A., 2002. Identification of animal fats via compound specific $\delta^{13}C$ values of individual fatty acids: assessments of results for reference fats and lipid extracts of archaeological pottery vessels, Documenta Praehistorica XXIX, 73-96.
Evershed, R.P., Payne, S., Sherratt, A.G., Copley, M.S., Coolidge, J., Urem-Kotsu, D., Kotsakis, K., Ozdogan, M., Ozdogan, A.E., Nieuwenhuyse, O., Akkermans, P.M.M.G., Bailey, D., Andeescu, R.-R., Campbell, S., Farid, S., Hodder, I., Yalman, N., Ozbasaran, M., Bicakci, E., Garfinkel, Y., Levy, T., Burton, M.M., 2008. Earliest date for milk use in the Near East and southeastern Europe linked to cattle herding, Nature 455, 528-531.
Evershed, R.P., Turner-Walker, G., Hedges, R.E.M., Tuross, N., Leyden, A., 1995. Preliminary Results for the Analysis of Lipids in Ancient Bone, Journal of Archaeological Science 22, 277-290.
Ficken, K.J., Street-Perrott, F.A., Perrott, R.A., Swain, D.L., Olago, D.O., Eglinton, G., 1998. Glacial/interglacial variation in carbon cycling revealed by molecular and isotope stratigraphy of Lake Nkunga, Mt. Kenya, East Africa, Organic Geochemistry 29, 1701-1719.
Franklin, W.L., 1983. Contrasting socioecologies of South America's wild camelids: the vicuña and the guanaco, American Society of Mammalogy Special publication 7, 573-628.
Gil, A., Zárate, M., Neme, G., 2005. Mid-Holocene paleoenvironments and the archeological record of southern Mendoza, Argentina, Quaternary International 132, 81-94.
Gregg, M.W., Banning, E.B., Gibbs, K., Slater, G.F., 2009. Subsistence practices and pottery use in Neolithic Jordan: molecular and isotopic evidence, Journal of Archaeological Science 36, 937-946.
Heusser, C.J., 1993. Palinología de la secuencia sedimentaria de la Cueva Traful I (provincia del Neuquén, República Argentina), Præhistoria 1, 206-208.
Heusser, C.J., Denton, G.H., Hauser, A., Andersen, B.G., Lowell, T.V., 1996. Water Fern (Azolla filiculoides Lam.) in Southern Chile as an Index of Paleoenvironment during Early Deglaciation, Arctic and Alpine Research 28, 148-155.
Heusser, C.J., Streeter, S.S., 1980. A Temperature and Precipitation Record of the past 16,000 Years in Southern Chile, Science 210, 1345-1347.
Howland, M.R., Corr, L.T., Young, S.M.M., Jones, V., Jim, S., Van Der Merwe, N.J., Mitchell, A.D., Evershed, R.P., 2003. Expression of the dietary isotope signal in the compound-specific δ13C values of pig bone lipids and amino acids, International Journal of Osteoarchaeology 13, 54-65.
Huang, Y., Shuman, B., Wang, Y., Thompson Webb III, Grimm, E.C., Jacobson Jr., G.L., 2006. Climatic and environmental controls on the variation of C3 and C4 plant abundances in central

Florida for the past 62,000 years, Palaeogeography, Palaeoclimatology, Palaeocology 237, 428-435.
Huang, Y., Street-Perrott, F.A., Perrott, R.A., Metzger, P., Eglinton, G., 1999. Glacial–interglacial environmental changes inferred from molecular and compound-specific $\delta^{13}C$ analyses of sediments from Sacred Lake, Mt. Kenya, Geochimica et Cosmochimica Acta 63, 1383-1404.
Jacob, J., Disnar, J.-R., Boussafir, M., Sifeddine, A., Turcq, B., Spadano Albuquerque, A.L., 2004. Major enviromental change recorded by lacustrine sedimentary organic matter since the last glacial maximum near the equator (Lagoa do Caçó, NE Brazil), Palaeogeography, Palaeoclimatology, Palaeocology 205, 183-197.
Jacob, J., Huang, Y., Disnar, J.-R., Sifeddine, A., Boussafir, M., Spadano Albuquerque, A.L., Turcq, B., 2007. Paleohydrological change during the last deglaciation in Northern Brazil, Quaternary Science Reviews 26, 1004-1015.
Jenny, B., Valero-Garcés, B.L., Villa, M., amp, x, nez, R., Urrutia, R., Geyh, M., Veit, H., 2002. Early to Mid-Holocene Aridity in Central Chile and the Southern Westerlies: The Laguna Aculeo Record (34°S), Quaternary Research 58, 160-170.
Jim, S., Ambrose, S.H., Evershed, R.P., 2004. Stable carbon isotopic evidence for differences in the dietary origin of bone cholesterol, collagen and apatite: implications for their use in palaeodietary reconstruction, Geochimica et Cosmochimica Acta 68, 61-72.
Lamy, F., Hebbeln, D., Röhl, U., Wefer, G., 2001. Holocene rainfall variability in southern Chile: a marine record of latitudinal shifts of the Southern Westerlies, Earth and Planetary Science Letters 185, 369-382.
León, R.J.C., Bran, D., Collantes, M., Paruelo, J.M., Soriano, A., 1998. Grandes unidades de vegetación de la Patagonia extra andina, Ecología Austral 8, 125-144.
Lucquin, A., March, J.R., 2003. Les méthodes de cuisson pré et proto historiques: le cas du bouilli, in: Frère, S. (Ed.), Le feu domestique et ses structures au néolithique et aux âges des métaux. Actes du colloque Bourg-en-bresse, Editions Monique Mergoil, Montagnac, pp. 127-143.
Llano, C., 2009. Photosynthetic Pathways, Spatial Distribution, Isotopic Ecology, and Implications for Pre-Hispanic Human Diets in Central-Western Argentina, International Journal of Osteoarchaeology 19, 130-143.
MacFadden, B.J., Cerling, C.E., Harris, J.M., Prado, J., 1999. Ancient latitudinal gradient of C3/C4 grasses interpreted from stable isotopes of New Word Pleistocene horse (*Equus*) teeth, Global Ecology Biogeography 8, 137-149.
MacFadden, B.J., Cerling, C.E., Prado, J., 1996. Cenozoic Terrestial Ecosystem Evolution in Argentina : Evidence from Carbon Isotopes of Fossil Mammal Teeth, Palaios 11, 319-327.
Maier, M.S., de Faria, D.L.A., Boschín, M.T., Parera, S.D., del Castillo Bernal, M.F., 2007. Combined use of vibrational spectroscopy and GC–MS methods in the characterization of archaeological pastes from Patagonia, Vibrational Spectroscopy 44, 182-186.
Makarewicz, C., Tuross, N., 2006. Foddering by Mongolian pastoralists is recorded in the stable carbon (δ13C) and nitrogen (δ15N) isotopes of caprine dentinal collagen, Journal of Archaeological Science 33, 862-870.
Mancini, M.V., Paez, M.M., Prieto, A.R., Stutz, S., Tonello, M.S., Vilanova, I., 2005. Mid-Holocene climatic variability reconstrution from pollen records (32°-52°S, Argentina), Quaternary International 132, 47-59.
March, J.R., 1995. Méthodes physiques et chimiques appliquées à l'étude des structures de combustion préhistoriques: l'approche par la chimie organique, Université de Paris I, Paris.
March, J.R., 1999. Chimie organique appliquee a l´etude des structures de combustion du site de Túnel I, Revue d'Archéometrie 23, 127-156.
March, J.R., Lucquin, A., 2006. About cooking and firing: Chemical analysis of fat residues from experimental and archaeological data. In in: Lovino, M.R. (Ed.), The Significance of Experimentation for the Interpretation of the Archaeological Processes: Methods, Problems and Projects, Colloque Section 1 BAR Archaeopress, Oxford, pp. 1-20.

March, R., In press. Searching for the functions of fire structures in Eynan (Mallaha) and their formation processes: a geochemical approach, in: Bar-Yosef, O., Valla, F.R. (Eds.), The Natufian Culture of the Levant II International Monographs in Prehistory, Ann Arbor.
March, R., Lucquin, A., Joly, D., Ferreri, J., Muhieddine, M., 2012. Processes of Formation and Alteration of Archaeological Fire Structures: Complexity Viewed in the Light of Experimental Approaches, Journal of Archaeological Method and Theory, 1-45. DOI 10.1007/s10816-10012-19134-10817.
Markgraf, V., 1983. Late and Postglacial Vegetational and Paleoclimatic Change in Subantartic and Arid Environments in Argentina, Palynology 7, 43-70.
Markgraf, V., Bradbury, J.P., Schwalb, A., Burns, S.J., Stern, C., Ariztegui, D., Gilli, A., Anselmetti, F.S., Stine, S., Maidana, N., 2003. Holocene palaeoclimates of southern Patagonia: limnological and environmental history of Lago Cardiel, Argentina, The Holocene 13, 581-591.
Markgraf, V., Iglesias, V., Whitlock, C., 2013. Late and postglacial vegetation and fire history from Cordón Serrucho Norte, northern Patagonia, Palaeogeography, Palaeoclimatology, Palaeoecology 371, 109-118.
Markgraf, V., Webb, R.S., Anderson, K.H., Anderson, L., 2002. Modern pollen/climate calibration for southern South America, Palaeogeography, Palaeoclimatology, Palaeoecology 181, 375-397.
Markgraf, V., Whitlock, C., Anderson, R.S., García, A., 2009. Late Quaternary vegetation and fire history in the northernmost *Notofagus* forest region: Mallín Vaca Lauquen, Neuquén Province, Argentina, Journal of Quaternary Science 24, 248-258.
McCarthy, R.D., Duthie, A.H., 1962. A rapid quantitative method for the separation of free fatty acids from other lipids, Journal of Lipids Reserch 3, 117-119.
Moreno, P.I., 1997. Vegetation and climate near Lago Llanquihue in the Chilean Lake District between 20200 and 9500 14C yr BP, Journal of Quaternary Science 12, 485-500.
Moreno, P.I., 2004. Millennial-scale climate variability in northwest Patagonia over the last 15 000 yr, Journal of Quaternary Science 19, 35-47.
Ortega, I.M., Franklin, W.L., 1995. Social Organization, Distribution and Movements of a Migratory Guanaco Population in the Chilean Patagonia, Revista Chilena de Historia Natural 68, 489-500.
Outram, A.K., Stear, N.A., Bendrey, R., Olsen, S., Kasparov, A., Zaibert, V., Thorpe, N., Evershed, R.P., 2009. The Earliest Horse Harnessing and Milking, Science 323, 1332-1335.
Pardiñas, U.F.J., Teta, P., 2008. Small Mammals and Paleoenvironments around the Pleistocene-Holocene Boundary in Patagonia, Current Research in the Pleistocene 25, 186-187.
Pardiñas, U.F.J., Teta, P., In press. Holocene stability and recent dramatic changes in micromammalian communities of northwestern Patagonia, Quaternary International (2012), , http://dx.doi.org/10.1016/j.quaint.2012.1008.1001.
Paruelo, J.M., Jobbagy, E.G., Oesterheld, M., Galluscio, R.A., Aguiar, M.R., 2007. The Grassland and Steppes of Patagonia and Río de la Plata Plains, in: Veblen, T.T., Young, K.R., Orme, A.R. (Eds.), The Physical Geography of South America, Oxford University Press, Oxford, pp. 233-249.
Paruelo, J.M., Jobbagy, E.G., Sala, O.E., Lauenroth, W.K., Burke, I.C., 1998. Funtional and Structural Convergence of Temperate Grassland and Shrubland Ecosystems, Ecological Applications 8, 194-206.
Pearson, A.K., Pearson, O.P., 1993. La fauna de mamíferos pequeños de Cueva Traful I, Argentina: pasado y presente, Præhistoria 1, 211-224.
Prieto, A.R., Stutz, S., 1996. Vegetación del Holoceno en el norte de la estepa patagónica: palinología de la Cueva Epullán Grande (Neuquén), Præhistoria 2, 267-277.
Puig, S., Videla, F., 1999. Dinámica poblacional y uso de habitat por el guanaco, in: González, B.P., Bas, F.M., Tala, C.G., Iriarte, A.W. (Eds.), Seminario. Manejo sustentable de la vicuña y el guanaco, Pontificia Universidad Católica de Chile, Santiago, pp. 57-65.

Puig, S., Videla, F., Cona, M.I., 1997. Diet and abundance of the guanaco (Lama guanicoeMüller 1776) in four habitats of northern Patagonia, Argentina, Journal of Arid Environments 36, 343-357.
Puig, S., Videla, F., Monge, S., Roig, V., 1996. Seasonal variations in guanaco diet (Lama guanicoeMüller 1776) and food availability in Northern Patagonia, Argentina, Journal of Arid Environments 34, 215-224.
Pyankov, V.I., Gunin, P.D., Tsoog, S., Black, C.C., 2000. C4 Plants in the Vegetation of Mongolia: Their Natural Occurrence and Geographical Distribution in Relation to Climate, Oecologia 123, 15-31.
Raedeke, K.J., 1979. Population Dynamics and Sociecology of the guanaco (*Lama guanicoe*) of Magallanes, Chile, University of Washington, Washington.
Read, J., Farquhar, G., 1991. Comparative Studies in Nothofagus (Fagaceae). I. Leaf Carbon Isotope Discrimination, Functional Ecology 5, 684-695.
Reimer, P., Baillie, M., Bard, E., Bayliss, A., Beck, J., Blackwell, P., Bronk Ramsey, C., Buck, C., Burr, G., Edwards, R., Friedrich, M., Grootes, P., Guilderson, T., Hajdas, I., Heaton, T., Hogg, A., Hughen, K., Kaiser, K., Kromer, B., McCormac, F., Manning, S., Reimer, R., Richards, D., Southon, J., Talamo, S., Turney, C., van der Plicht, J., Weyhenmeyer, C., 2009. IntCal09 and Marine09 Radiocarbon Age Calibration Curves, 0–50,000 Years cal BP, Radiocarbon 51, 1111-1150
Rommerskirchen, F., Eglinton, G., Dupont, L., Güntner, U., Wenzel, C., Rullkötter, J., 2003. A north to south transect of Holocene southeast Atlantic continental margin sediments: Relationship between aerosol transport and compound-specific $\delta^{13}C$ land plant biomarker and pollen records, Geochemistry Geophysics Geosystems 4, 1101.
Rommerskirchen, F., Eglinton, G., Dupont, L., Rullkötter, J., 2006. Glacial/interglacial changes in southern Africa: Compound-specific $\delta^{13}C$ land plant biomarker and pollen records from southeast Atlantic continental margin sediments, Geochemistry Geophysics Geosystems 7, Q08010.
Ruess, L., Chamberlain, P.M., 2010. The fat that matters: Soil food web analysis using fatty acids and their carbon stable isotope signature, Soil Biology & Biochemistry 42, 1898-1910.
San Martín, F., Bryant, F.C., 1988. Comparación de las tasas de pasaje de la fase líquida y de la fase sólida en el tracto digestivo de llama y ovino, in: San Martín, F., Bryant, F.C. (Eds.), nvestigaciones sobre pastos y forrajes de Texas Tech University en el Perú, Texas Tech University, Lubbock, pp. 84–93.
Skinner, H.R., Hanson, J.D., Hutchinson, G.L., Schuman, G., 2002. Response of C_3 and C_4 Grasses to Supplemental Summer Precipitation, Journal of Range Management 55, 517-522.
Spangenberg, J.E., Jacomet, S., Schibler, J., 2006. Chemical analyses of organic residues in archaeological pottery from Arbon Bleiche 3, Switzerland – evidence for dairying in the late Neolithic, Journal of Archaeological Science 33, 1-13.
Stine, S., Stine, M., 1990. A record from Lake Cardiel of climate change in southern South America, Nature 345, 705-708.
Stott, A.W., Davies, E., Evershed, R.P., Tuross, N., 1997. Monitoring the Routing of Dietary and Biosynthesised Lipids Through Compound – Specific Stable Isotope (δ13C) Measurements at Natural Abundance, Naturwissenschaften 84, 82-86.
Stutz, S., 1994. Análisis palinológico de los sitios arqueológicos Cueva Epullán Grande y Cueva Epullán Chica (Neuquén), Revista del Museo de Historia Natural de San Rafael XIV, 316-318.
Tornero, C., Sana, M., 2011. Integrating Stable Isotopes to the Study of the Origin of Management Strategies for Domestic Animals: $\delta^{13}C$ and $\delta^{18}O$ Results from Bioapatite Enamel of Cattle from the Tell Halula Site, Syria (7800-7000 BC), in: Turbanti-Memmi, I. (Ed.), Proceedings of the 37th International Symposium on Archaeometry, Springer-Verlag Berlin Heidelberg, pp. 435-440.
Veblen, T.T., Lorenz, D.C., 1988. Recent Vegetation Changes along the Forest/Steppe Ecotone of Northern Patagonia, Annals of the Association of American Geographers 78, 93-111.

Veit, H., 1996. Southern Westerlies during the Holocene deduced from geomorphological and pedological studies in the Norte Chico, Northern Chile (27–33°S), Palaeogeography, Palaeoclimatology, Palaeoecology 123, 107-119.
Villalba, R., 1990. Climatic Fluctuactions in Northern Patagonia during the Last 1000 Years as Inferred from Tree-Ring Records, Quaternary Research 34, 346-360.
Villalba, R., 1994. Fluctuaciones climáticas medias de América del Sur durante los últimos 1000 años: sus relaciones con la Oscilación del Sur, Revista Chilena de Historia Natural 67, 453-461.
Villarosa, G., Outes, V., Hajduk, A., Crivelli Montero, E., Sellés, D., Fernández, M., Crivelli, E., 2006. Explosive volcanism during the Holocene in the Upper Limay River Basin: The effects of ashfalls on human societies, Northern Patagonia, Argentina, Quaternary International 158, 44-57.
Wheeler, J.C., 1991. Origen, evolución y status actual, in: Fernández-Baca, S. (Ed.), Avances y perspectivas del conocimiento de los camélidos sudamericanos, FAO, Santiago de Chile, pp. 11-48.
Whitlock, C., Bianchi, M.M., Patrick, J.B., Markgraf, V., Marlon, J., McCoy, N., 2006. Postglacial vegetation, climate, and fire history along the east side of the Andes (lat 41-42.5°S), Argentina, Quaternary International 66, 187-201.
Widga, C., Walker, J.D., Stockli, L.D., 2010. Middle Holocene Bison diet and mobility in the Eastern Great Plains (USA) base on $\delta^{13}C$ $\delta^{18}O$, and 87Sr/86Sr analyses of tooth enamel carbonate, Quaternary Research 73, 449-463.
Zech, M., Zech, R., Morrás, H., Moretti, L., Glaser, B., Zech, W., 2009. Late Quaternary environmental changes in Misiones, subtropical NE Argentina, deduced from multi-proxy geochemical analyses in a palaeosol-sediment sequence, Quaternary International 196, 121-136.
Zhang, Z., Zhao, M., Eglinton, G., Lu, H., Huang, C.-Y., 2006. Leaf wax lipids as paleovegetational and paleoenvironmental proxies for the Chinese Loess Plateau over the last 170 kyr, Quaternary Science Reviews 25, 575-594.

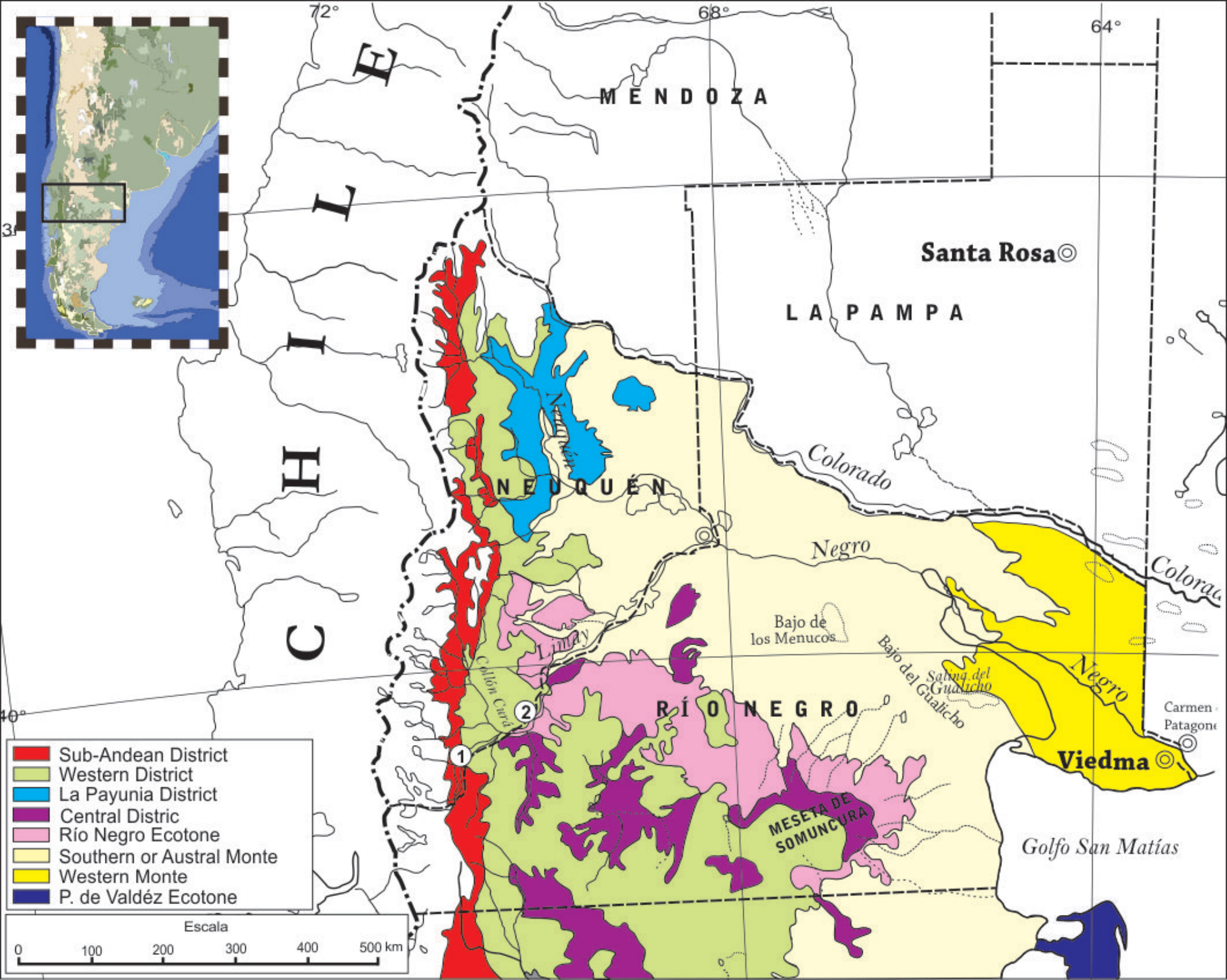
72°
68°
64°
CHILE
MENDOZA
Santa Rosa
LA PAMPA
NEUQUÉN
Neuquén
Colorado
Negro
Bajo de los Menucos
Bajo del Gualicho
Salina del Gualicho
Limay
Collón Curá
RÍO NEGRO
MESETA DE SOMUNCURA
Viedma
Carmen de Patagones
Golfo San Matías
1
2
Sub-Andean District
Western District
La Payunia District
Central Distric
Río Negro Ecotone
Southern or Austral Monte
Western Monte
P. de Valdéz Ecotone
Escala
0
100
200
300
400
500 km

A

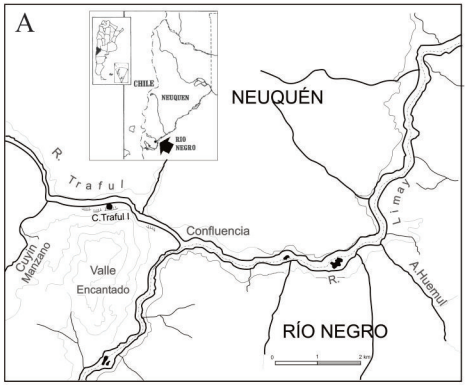

B

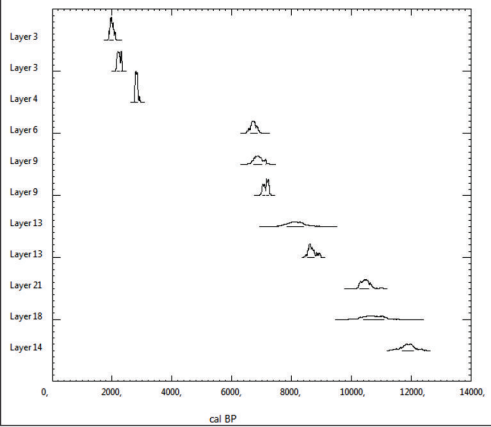

C

CULTURAL UNITS AND CRONOLOGY OF TRAFUL I

YEARS AP	LAYERS	CULTURALS UNITS
	1 2	Final occupations
2.230 ± 40 2.720 ± 40	3 3A 3A' 4	Component IIB
	5	Tephra
	6	Sterile
6.030 ± 115 6.240 ± 60	7 8 9	Component IIA Confluence
7.308 ± 285 7.850 ± 70	10 11 11' 12 13 14 15	Component I Traful
	16 17	Sterile
9.430 ± 230 9.285 ± 105	18 19 20 21	First occupations
	Bed rock	

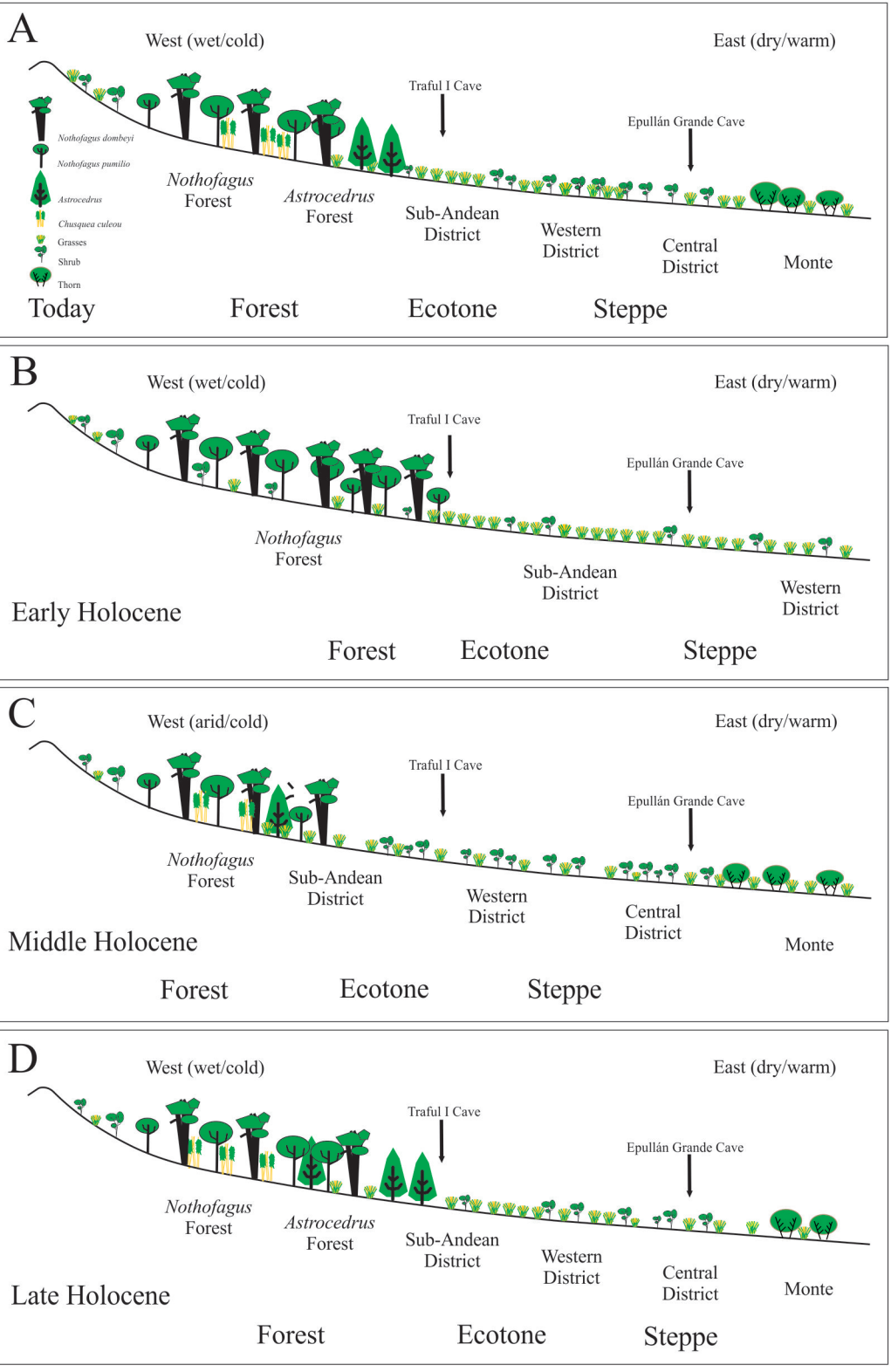
A
West (wet/cold)
East (dry/warm)
Nothofagus dombeyi
Nothofagus pumilio
Astrocedrus
Chusquea culeou
Grasses
Shrub
Thorn
Traful I Cave
Epullán Grande Cave
Nothofagus Forest
Astrocedrus Forest
Sub-Andean District
Western District
Central District
Monte
Today
Forest
Ecotone
Steppe
B
West (wet/cold)
East (dry/warm)
Traful I Cave
Epullán Grande Cave
Nothofagus Forest
Sub-Andean District
Western District
Early Holocene
Forest
Ecotone
Steppe
C
West (arid/cold)
East (dry/warm)
Traful I Cave
Epullán Grande Cave
Nothofagus Forest
Sub-Andean District
Western District
Central District
Monte
Middle Holocene
Forest
Ecotone
Steppe
D
West (wet/cold)
East (dry/warm)
Traful I Cave
Epullán Grande Cave
Nothofagus Forest
Astrocedrus Forest
Sub-Andean District
Western District
Central District
Monte
Late Holocene
Forest
Ecotone
Steppe

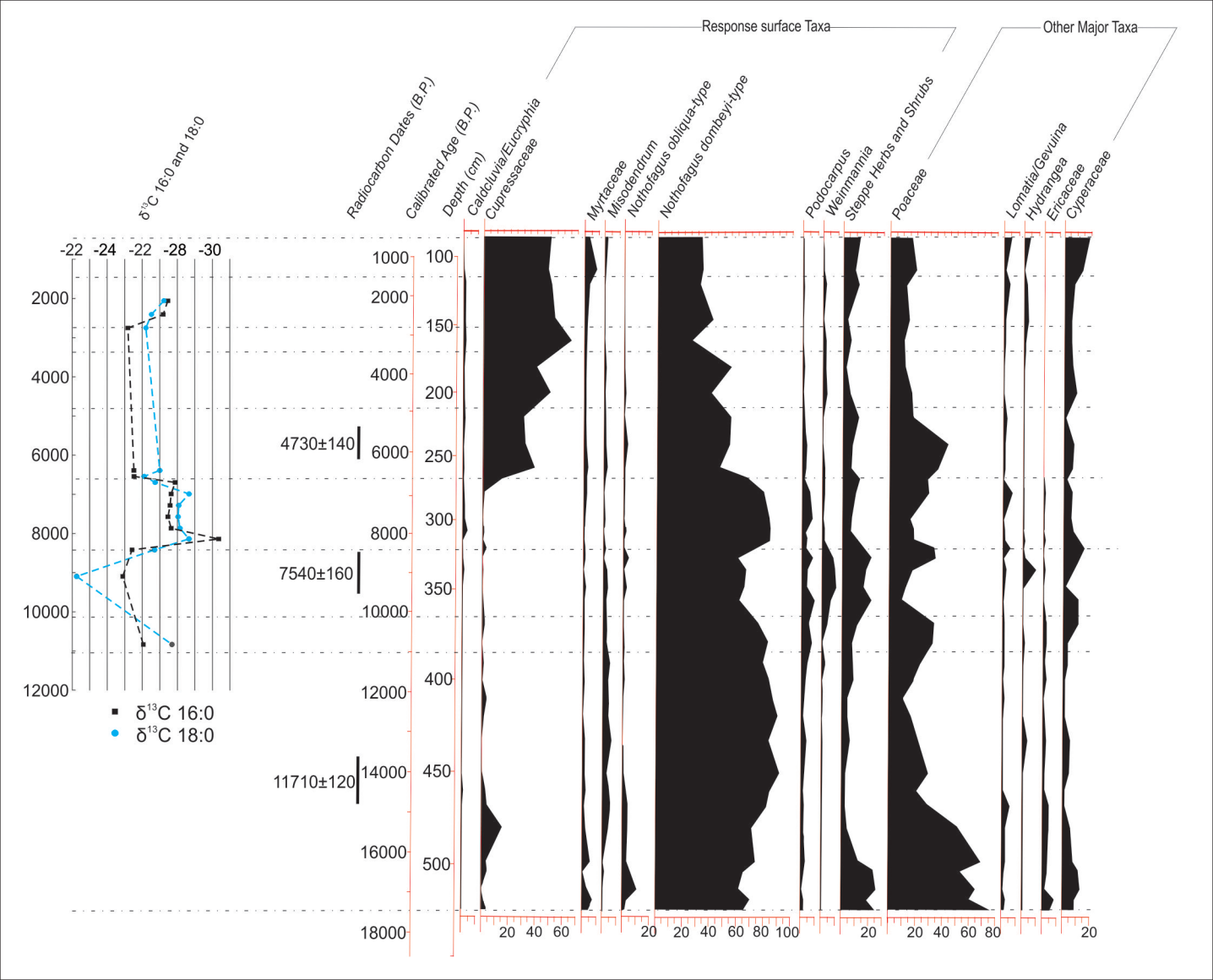
Response surface Taxa
Other Major Taxa
δ13C 16:0 and 18:0
Radiocarbon Dates (B.P.)
Calibrated Age (B.P.)
Depth (cm)
Caldcluvia/Eucryphia
Cupressaceae
Myrtaceae
Misodendrum
Nothofagus obliqua-type
Nothofagus dombeyi-type
Podocarpus
Weinmannia
Steppe Herbs and Shrubs
Poaceae
Lomatia/Gevuina
Hydrangea
Ericaceae
Cyperaceae
-22 -24 -22 -28 -30
2000
4000
6000
8000
10000
12000
δ13C 16:0
δ13C 18:0
4730±140
7540±160
11710±120
1000
2000
4000
6000
8000
10000
12000
14000
16000
18000
100
150
200
250
300
350
400
450
500
20 40 60
20 20 40 60 80 100
20
20 40 60 80
20

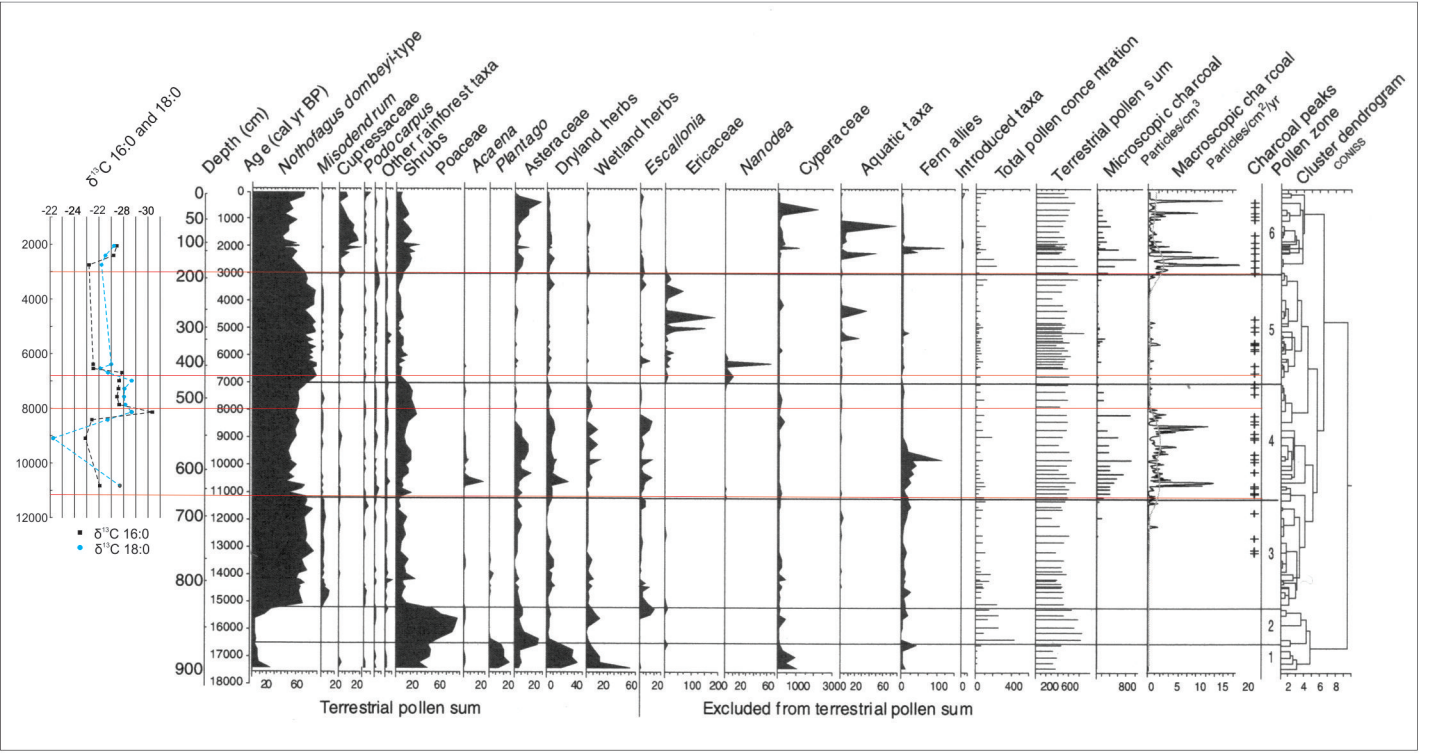
δ13C 16:0 and 18:0
-22 -24 -22 -28 -30
δ13C 16:0
δ13C 18:0
Depth (cm)
Age (cal yr BP)
Nothofagus dombeyi-type
Misodendrum
Cupressaceae
Podocarpus
Other rainforest taxa
Shrubs
Poaceae
Acaena
Plantago
Asteraceae
Dryland herbs
Wetland herbs
Escallonia
Ericaceae
Nanodea
Cyperaceae
Aquatic taxa
Fern allies
Introduced taxa
Total pollen concentration
Terrestrial pollen sum
Microscopic charcoal
Particles/cm3
Macroscopic charcoal
Particles/cm2/yr
Charcoal peaks
Pollen zone
Cluster dendrogram
CONISS
Terrestrial pollen sum
Excluded from terrestrial pollen sum

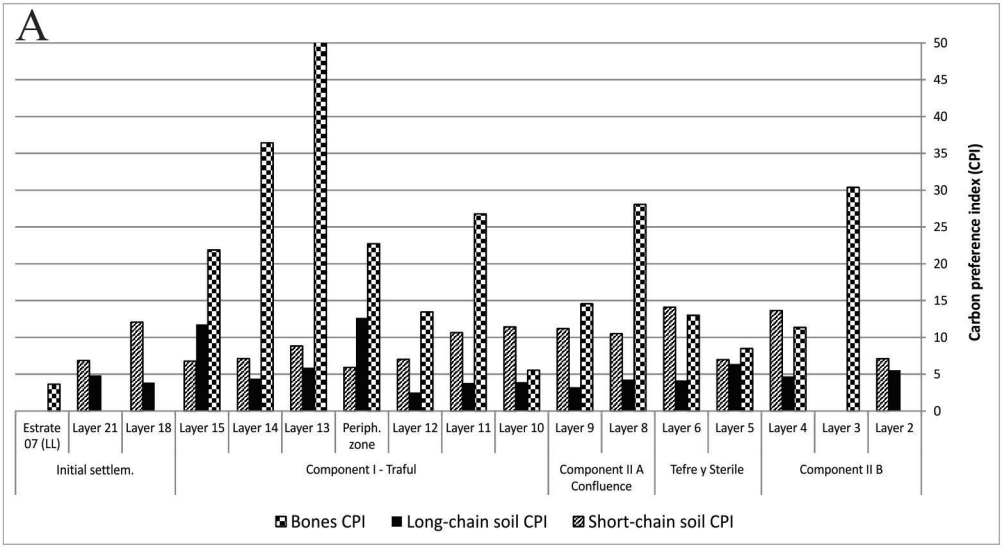
A
50
45
40
35
30
25
20
15
10
5
0
Carbon preference index (CPI)
Estrate 07 (LL)
Layer 21
Layer 18
Layer 15
Layer 14
Layer 13
Periph. zone
Layer 12
Layer 11
Layer 10
Layer 9
Layer 8
Layer 6
Layer 5
Layer 4
Layer 3
Layer 2
Initial settlem.
Component I - Traful
Component II A Confluence
Tefre y Sterile
Component II B
Bones CPI
Long-chain soil CPI
Short-chain soil CPI

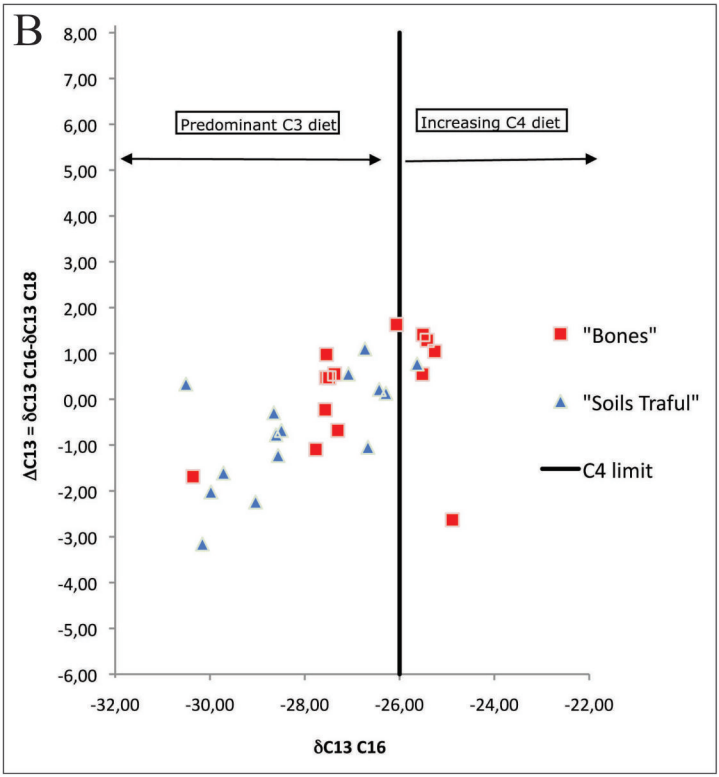
B
8,00
7,00
6,00
5,00
4,00
3,00
2,00
1,00
0,00
-1,00
-2,00
-3,00
-4,00
-5,00
-6,00
ΔC13 = δC13 C16-δC13 C18
Predominant C3 diet
Increasing C4 diet
"Bones"
"Soils Traful"
C4 limit
-32,00
-30,00
-28,00
-26,00
-24,00
-22,00
δC13 C16

Table 1

Values of δ13C16 and δ13C18. weight. mass FAME and CPI

Layers	Bones		Soil		Bones				Soils	
	δ13C16 ‰	δ13C18 ‰	δ13C16 ‰	δ13C18 ‰	Weight (g)	Mass FAME (ug/g) C16	Mass FAME (ug/g) C18	CPI	Long-chain CPI	Short-chain CPI
Layer 2			-26.66	-25.61					5.555	7.103
Layer 3	-27.56	-27.34	-25.63	-26.40	1.502.911	0.311	0.220	30.39	6.397	6.972
Tephra	-27.30	-26.62	-28.56	-27.34	1.228.706	0.614	0.382	8.50	4.712	13.640
Layer 4	-25.25	-26.30	-26.29	-26.42	855.129	0.487	0.304	11.37	4.165	14.091
Layer 6	-25.50	-26.92	-30.50	-30.83	135.954	0.803	0.605	13.00	4.266	10.506
Layer 8	-25.51	-26.06	-29.98	-27.96	677.837	0.477	0.461	28.08	3.247	11.201
Layer 9	-27.76	-26.67	-28.49	-27.81	717.619	0.703	0.727	14.57	3.919	11.422
Layer 10	-27.54	-28.51	-28.65	-28.36	608.949	2.925	1.476	5.56	3.814	10.645
Layer 11	-27-48	-27.95	-30.16	-27.00	260.389	1.354	1.997	26.79	2.522	7.013
Layer 12	-27.37	-27.92	-29.04	-26.80	592.368	1.794	1.566	13.45	12.653	5.921
Periph. zone	-27.54	-28.02	-28.60	-27.83	717.373	1.358	1.538	22.73	5.901	8.833
Layer 13	-30.35	-28.66	-29.72	-28.11	1.982.431	1.645	0.745	77.33	4.394	7.118
Layer 14	-25.41	-26.70	-26.73	-27.83	132.948	0.177	0.226	36.43	11.768	6.769
Layer 15	-24.88	-22.25			536.188	0.458	0.571	21.88		
Layer 18			-26.43	-26.65					3.860	12.079
Layer 21			-27.08	-27.63					4.844	6.857
Estrate 07 (LL)	-26.06	-27.69			524.567	1.863	1.333	3.65		

Table 2
Saturated, unsaturated and branched fatty acid sample compositions

		Last occup.	Component IIB				Tefra		Hiatus		Component IA- Confluencia				
		Layer 2	Layer 3		Layer 4		Layer 5		Layer 6		Layer 7	Layer 8		Layer 9	
		Soil	Soil	Bone	Soil	Bone	Soil	Bone	Soil	Bone	Soil	Soil	Bone	Soil	Bone
Nonanoic acid	**C9:0**	X					X				X				
Decanoic acid	**C10:0**	X	X				X		X		X				
Undecanoic acid	**C11:0**	X	X				X		X		X				
Undecanoic acid, 10-methyl-, methylester			X												
Dodecanoic acid	**C12:0**	X	X		X		X		X		X	X		X	
Dodecanoic acid, 4-methyl-, methylester			X												
Dodecanoic acid, 10-methyl-, methyl ester		X	X												
Tridecanoic acid	**C13:0**	X	X		X		X		X		X	X		X	
Tetradecanoic acid, 12-methyl-, methyl ester							X					X		X	
Hexadecanoic acid, 15-methyl-, methyl ester									X						
Tridecanoic acid, 4,8,12-trimethyl- methylester															
Methyl tetradecanoate	**C14:0**	X	X		X	O	X	O	X	O	X	X	O	X	O
Tetradecanoic acid, 12-methyl-, methyl ester		X	X		X		X		X		X	X		X	
Methy Z-11-tetradecenoate	C15:1ω11	X													
Pentadecanoic acid	**C15:0**	X	X	O	X	O	X	O	X	O	X	X	O	X	O
Pentadecanoic acid, 14-methyl-, methyl ester		X	X		X				X		X	X		X	
7-Hexadecenoic acid	C16:1ω7	X	X		X		X		X		X	X			
9-Hexadecenoic acid	C16:1ω9					O								X	
11-Hexadecenoic acid	C16:1ω11	X	X				X				X			X	
Hexadecanoic acid	**C16:0**	X	X	O	X	O	X	O	X	O	X	X	O	X	O
Hexadecanoic acid, 14-methyl-, methyl ester		X	X		X				X		X	X		X	
Hexadecanoic acid, 15-methyl-, methyl ester															
Heptadecanoic acid	**C17:0**	X	X	O	X	O	X	O	X	O	X	X	O	X	O
Heptadecanoic acid, 10-methyl-, methyl ester		X	X		X		X								
Pentadecanoic acid, 14-methyl-, methyl ester															
8,11-Octadecadienoic acid	C18:2ω8,11											X			
9,12-Octadecadienoic acid	C18:2ω9,12	X	X				X							X	
9,15-Octadecadienoic acid	C18:2ω9,15				X										
11,14-Octadecadienoic acid	C18:2ω11,14														
14,17-Octadecadienoic acid	C18:2ω14,17														
6-Octodecenoic acid	C18:1ω6														
8-Octodecenoic acid	C18:1ω8		X								X				
9-Octodecenoic acid	C18:1ω9	X			X		X					X		X	
10-Octodecenoic acid	C18:1ω10	X				O	X		X						
11-Octodecenoic acid	C18:1ω11														
16-Octodecenoic acid	C18:1ω16											X			
Octadecanoic acid	**C18:0**	X	X	O	X	O	X	O	X	O	X	X	O	X	O
Octadecanoic acid, 10-methyl-, methyl ester		X	X				X		X			X		X	
Octadecanoic acid, 17-methyl-, methyl ester									X			X		X	
8,11-Octodecadienoic acid	C19:2ω8,11	X													
7,10-Octodecadienoic acid	C19:2ω7,10		X		X										
11-Nonadecenoic acid	C19:1ω11				X										
10-Nonadecenoic acid	C19:1ω10	X	X						X						
Nonadecanoic acid	**C19:0**	X	X		X		X		X		X	X		X	
11-Etcosenoic acid	C20:1		X		X		X		X		X			X	
Etcosanoic acid	**C20:0**	X	X				X		X	O	X	X	O	X	
Octodecanoic acid, 17-oxo-, methylester												X			
Hexadecanoic acid, 14-methyl methylester		X													
Heneicosanoic acid	**C21:0**	X	X				X		X			X		X	
13-Docosenoic acid	C22:1ω13	X	X		X		X				X	X		X	
Docosanoic acid	**C22:0**	X	X		X		X		X	O	X	X	O	X	
Tricosanoic acid	**C23:0**	X	X		X		X		X		X	X		X	
Tetracosanoic acid	**C24:0**	X	X		X		X		X	O	X	X	O	X	
13-Docosenamide, (Z)-		X	X		X		X		X			X		X	
Pentacosanoic acid	**C25:0**	X	X		X		X		X		X	X		X	
Hexacosanoic acid	**C26:0**	X	X		X		X		X			X		X	
7-Oxo-5-cholesten-"beta-ylbenzoate											X				
Heptacosanoic acid	**C27:0**	X	X		X		X					X		X	
Octacosanoic acid	**C28:0**	X	X		X		X					X		X	
Nonacosanoic acid	**C29:0**		X		X		X							X	
Triacontanoic acid	**C30:0**		X		X		X							X	
Henatriacontanoic acid	**C31:0**		X												
Dotriacontanoic acid	**C32:0**		X		X										

X presence in soils, O presence in bones

Table 2 (cont.)
Saturated, unsaturated and branched fatty acid sample compositions

		Component I - Traful													First occup.		LL
		Layer 10		Layer 11		Layer 12		Pe. Zone	Layer 13		Layer 14		Layer 15	Layer 18	Layer 21	Est. 07
		Soil	Bone	Soil	Bone	Soil	Bone	Bone	Soil	Bone	Soil	Bone	Bone	Soil	Soil	Bone
Nonanoic acid	**C9:0**			X		X			X		X					
Decanoic acid	**C10:0**			X		X			X		X					
Undecanoic acid	**C11:0**	X		X		X			X		X					
Undecanoic acid, 10-methyl-, methylester																
Dodecanoic acid	**C12:0**	X		X		X			X		X			X	X	
Dodecanoic acid, 4-methyl-, methylester																
Dodecanoic acid, 10-methyl-, methyl ester		X														
Tridecanoic acid	**C13:0**	X		X		X			X		X			X	X	
Tetradecanoic acid, 12-methyl-, methyl ester		X		X		X			X		X			X		
Hexadecanoic acid, 15-methyl-, methyl ester																
Tridecanoic acid, 4,8,12-trimethyl- methylester				X												
Methyl tetradecanoate	**C14:0**	X	O	X	O	X	O	O	X	O	X	O	O	X	X	
Tetradecanoic acid, 12-methyl-, methyl ester		X				X			X		X			X	X	
Methy Z-11-tetradecenoate	C15:1ω11															
Pentadecanoic acid	**C15:0**	X	O	X	O	X	O	O	X	O	X	O	O	X	X	
Pentadecanoic acid, 14-methyl-, methyl ester		X		X		X			X		X				X	
7-Hexadecenoic acid	C16:1ω7	X							X		X	O		X	X	
9-Hexadecenoic acid	C16:1ω9	X		X		X								X		
11-Hexadecenoic acid	C16:1ω11			X		X			X		X				X	
Hexadecanoic acid	**C16:0**	X	O	X	O	X	O	O	X	O	X	O	O	X	X	O
Hexadecanoic acid, 14-methyl-, methyl ester		X		X		X			X							
Hexadecanoic acid, 15-methyl-, methyl ester		X												X		
Heptadecanoic acid	**C17:0**	X	O	X	O	X	O	O		O	X	O	O	X	X	O
Heptadecanoic acid, 10-methyl-, methyl ester		X				X									X	
Pentadecanoic acid, 14-methyl-, methyl ester				X							X					
8,11-Octadecadienoic acid	C18:2ω8,11			X							X					
9,12-Octadecadienoic acid	C18:2ω9,12					X										
9,15-Octadecadienoic acid	C18:2ω9,15	X													X	
11,14-Octadecadienoic acid	C18:2ω11,14													X		
14,17-Octadecadienoic acid	C18:2ω14,17								X							
6-Octodecenoic acid	C18:1ω6										X					
8-Octodecenoic acid	C18:1ω8													X		
9-Octodecenoic acid	C18:1ω9					X								X		
10-Octodecenoic acid	C18:1ω10	X		X		X			X		X	O			X	

Table 2 (cont.)
Saturated, unsaturated and branched fatty acid sample compositions

		Component I - Traful												First occup.		LL
		Layer 10		Layer 11		Layer 12		Pe. Zone	Layer 13		Layer 14		Layer 15	Layer 18	Layer 21	Est. 07
		Soil	Bone	Soil	Bone	Soil	Bone	Bone	Soil	Bone	Soil	Bone	Bone	Soil	Soil	Bone
11-Octodecenoic acid	C18:1ω11			X												
16-Octodecenoic acid	C18:1ω16														X	
Octadecanoic acid	**C18:0**	X	O	X	O	X	O	O	X	O	X	O	O	X	X	O
Octadecanoic acid, 10-methyl-, methyl ester											X					
Octadecanoic acid, 17-methyl-, methyl ester		X												X		
8,11-Octodecadienoic acid	C19:2ω8,11															
7,10-Octodecadienoic acid	C19:2ω7,10															
11-Nonadecenoic acid	C19:1ω11															
10-Nonadecenoic acid	C19:1ω10	X														
Nonadecanoic acid	**C19:0**	X		X		X			X		X			X	X	
11-Etcosenoic acid	C20:1	X		X		X			X		X			X	X	
Etcosanoic acid	**C20:0**	X		X	O	X	O	O	X		X	O	O	X	X	
Octodecanoic acid, 17-oxo-, methylester																
Hexadecanoic acid, 14-methyl methylester																
Heneicosanoic acid	**C21:0**	X		X		X			X		X			X	X	
13-Docosenoic acid	C22:1ω13	X		X		X			X		X			X	X	
Docosanoic acid	**C22:0**	X		X	O	X	O	O	X		X	O	O	X	X	
Tricosanoic acid	**C23:0**	X		X		X			X		X			X	X	
Tetracosanoic acid	**C24:0**	X		X	O	X	O	O	X		X	O		X	X	
13-Docosenamide, (Z)-		X		X		X			X		X			X	X	
Pentacosanoic acid	**C25:0**	X		X		X			X		X			X	X	
Hexacosanoic acid	**C26:0**	X		X		X			X		X			X	X	
7-Oxo-5-cholesten-"beta-ylbenzoate																
Heptacosanoic acid	**C27:0**	X		X		X			X		X			X	X	
Octacosanoic acid	**C28:0**	X		X		X			X		X			X	X	
Nonacosanoic acid	**C29:0**	X		X		X										
Triacontanoic acid	**C30:0**	X		X		X			X						X	
Henatriacontanoic acid	**C31:0**	X														
Dotriacontanoic acid	**C32:0**	X		X		X			X							

X presence in soils, O presence in bones

Table 3
R Pearson values $p > 0.05$

	δ13C16	δ13C18	Mass FAME (ug/g) C16	Mass FAME (ug/g) C18	CPI
δ13C16		0,664	-0,462		
δ13C18				-0,480	
Peso (g)	-0,376	-0,198	-0,274	-0,606	0,636
CPI	-0,533	-0,159	-0,123	-0,186	